Dalton Transactions

Accepted Manuscript

ROYAL SOCIETY OF CHEMISTRY

www.rsc.org/dalton

Journal Name

RSCPublishing

ARTICLE

Reactivity of Bis(organoamino)phosphanes with Magnesium(II) Compounds.

Cite this: DOI: 10.1039/xoxxoooooox

Jan Vrána,[a] Roman Jambor,[a] Aleš Růžička,[a] Mercedes Alonso,[b] Frank De Proft,[b] Antonín Lyčka[c] and Libor Dostál*[a]

Received ooth January 2012,
Accepted ooth January 2012

DOI: 10.1039/xoxxoooooox

www.rsc.org/

Reactivity of three phosphanes PhP(NHR)$_2$ [R = *t*-Bu (**1**), Ph (**2**)] and PhP(NEt$_2$)(NHDip) (**3**) (where Dip = 2,6-*i*-Pr$_2$C$_6$H$_3$) with *n*-Bu$_2$Mg and MeMgBr is presented. In the case of **1**, the reaction with *n*-Bu$_2$Mg gave [PhP(NH*t*-Bu)(N*t*-Bu)]Mg(*n*-Bu) (**4**) and [PhP(NH*t*-Bu)(N*t*-Bu)]$_2$Mg (**5**) depending on the stoichiometry. The treatment of **1** with MeMgBr led to the phosphinate [Ph(H)P(N*t*-Bu)$_2$]$_2$Mg (**7**) as a result of both the NH→PH tautomeric transformation and elimination of MgBr$_2$ from non-isolable intermediate [PhP(NH*t*-Bu)(N*t*-Bu)]MgBr(THF) (**6**). Phosphane **2** reacted with *n*-Bu$_2$Mg in 1:1 molar ratio under formation of {[PhP(NPh)$_2$]$_2$Mg(THF)$_2$}$_2$ (**8**), but analogous reaction in 2:1 molar ratio yielded phosphinate [Ph(H)P(NPh)$_2$]$_2$Mg(THF) (**9**). Heteroleptic compound [Ph(H)P(NPh)$_2$]MgBr(THF)$_2$ (**10**) was obtained by the reaction of **2** with MeMgBr. Finally, reaction of **3** with *n*-Bu$_2$Mg and MeMgBr produced compounds [PhP(NEt$_2$)(NDip)]$_2$Mg (**11**) and {[PhP(NEt$_2$)(NDip)$_2$]Mg(*μ*-Br)(THF)}$_2$ (**12**), respectively. All products were characterized by the help of ^{1}H, ^{13}C{^{1}H} and ^{31}P NMR spectroscopy and except for **4** and **6** molecular structures were determined using single-crystal X-ray diffraction analysis. In addition, a theoretical study on plausible isomers of **10** was performed to provide additional evidence for the presence of a *syn*- and *anti*- isomer in dynamic equilibrium in solution of **10**.

Introduction

The chemistry of electron rich anionic amido- ligands, which are able to close strained four-membered chelating ring with a central atom, is very rich and miscellaneous (Figure 1). Their ligand backbones may be easily tuned from both steric and electronic point of view by a simple selection of appropriate R and R´ groups (Figure 1). Prominent examples include amidinates (**A**),[1] guanidinates (**B**)[1,2] and boramidinates (**C**).[3] Some attention has also been devoted to bulky sila- substituted amides (**D**).[4] These ligands found widespread applications in coordination chemistry of both transition metals and main group elements.[1-4] In contrast, the chemistry of phosphorus analogues i.e. amido(amino)phosphanes (**E**), bis(amido)phosphanes (**F**) or bis(imino)phosphinates (**G**) seems to be significantly less developed[5] in spite of the fact that their backbones contain ^{31}P NMR active nuclei perfectly suited for the monitoring of studied reactions. Furthermore, the presence of the phosphorus atom allows to switch between +III and +V oxidation state. In this regard, it has been demonstrated that bis(amino)phosphanes (and related deprotonated species) are under certain circumstances liable to NH→PH tautomeric transformation (Scheme 1) leading to amino(imino)phosphoranes (or bis(imino)phosphinates), thereby proving a high synthetic potential of such ligand-precursors.[6]

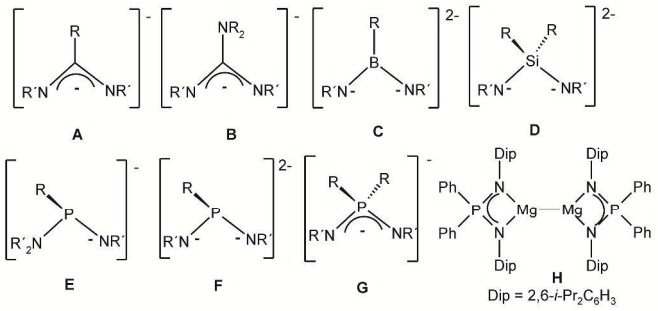

Figure 1 Structures of discussed ligands and a magnesium(I) dimer

Recently, we have successfully applied this synthetic strategy in the case of aluminum(III) complexes.[7] We report herein on the reactivity of analogous phosphanes **1-3** (Figure 2) with magnesium(II) compounds. There exists a number of magnesium(II) amides containing a P-N linkage in the ligand backbone,[8] but there is only a few structurally authenticated magnesium bis(imino)phosphinates.[9]

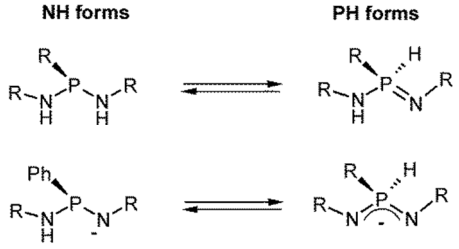

Scheme 1 Possible tautomeric forms of discussed compounds.

As an important contribution, Stasch has very recently succeeded in preparation of a dimeric magnesium(I) compound $[Ph_2P(NDip)_2Mg]_2$ stabilized the bis(imino)phosphinate (**H**).[10] The main aim of this work is to further develop the field of main group element complexes stabilized by ligands of the type **E**, **F, G** and to study a possible utilization NH→PH tautomerism (Scheme 1) for synthetic purposes.

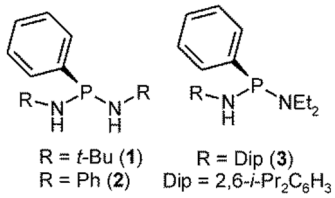

Figure 2 Structures of studied phosphanes **1**–**3**.

Results and Discussion

Syntheses and NMR studies

Starting phosphanes $PhP(NHR)_2$ [R = *t*-Bu (**1**), Ph (**2**)][11] were synthesized according to the literature procedures, while $PhP(NEt_2)(NHDip)$ (**3**) was prepared by the reaction of PhP(NHDip)(Cl)[12] with two molar equivalents of Et_2NH. **3** was isolated as a white solid in good yield of 91 % and characterized by the help of ^1H, $^{13}C\{^1H\}$ NMR spectroscopy (see the Experimental section). The ^{31}P NMR spectrum of **3** revealed a singlet at 82.5 ppm. The reactivity of titled phosphanes **1**-**3** with *n*-Bu_2Mg and MeMgBr differs and thus is discussed separately for each phosphane.

The reaction of **1** with *n*-Bu_2Mg gave, depending on the stoichiometry (Scheme 2), compounds [PhP(NH*t*-Bu)(N*t*-Bu)]Mg(*n*-Bu) (**4**) and $[PhP(NHt\text{-}Bu)(Nt\text{-}Bu)]_2Mg$ (**5**) as the result of evolution of one or two equivalents of *n*-butane. Both compounds were isolated as colourless crystals in 35% and 52% yield, respectively, which are well soluble both in aliphatic and aromatic solvents. The ^1H spectra showed two signals for magnetically non-equivalent *t*-Bu groups at 0.88 and 1.71 ppm for **4** and 1.05 and 1.57 ppm for **5** and one signal for the N*H* moiety at 1.86 ppm (**5**) (in the case of **4** this resonance is overlapped by the signals of *n*-Bu fragment). Similarly, two sets of signals for *t*-Bu groups were observed in the corresponding $^{13}C\{^1H\}$ NMR spectra, thereby proving the structure of **4** and **5**. The ^{31}P NMR spectra of **4** and **5** revealed signals at 88.3 and 92.5 ppm, respectively, both significantly shifted in comparison with the starting phosphane **1** [$\delta(^{31}P)$ = 41.6 ppm]. Recently, we have demonstrated that related aluminum amide $[PhP(NHt\text{-}Bu)(Nt\text{-}Bu)]AlMe_2$ smoothly underwent a tautomeric hydrogen shift upon heating with quantitative formation of the phosphinate $[Ph(H)P(Nt\text{-}Bu)_2]AlMe_2$.[7]

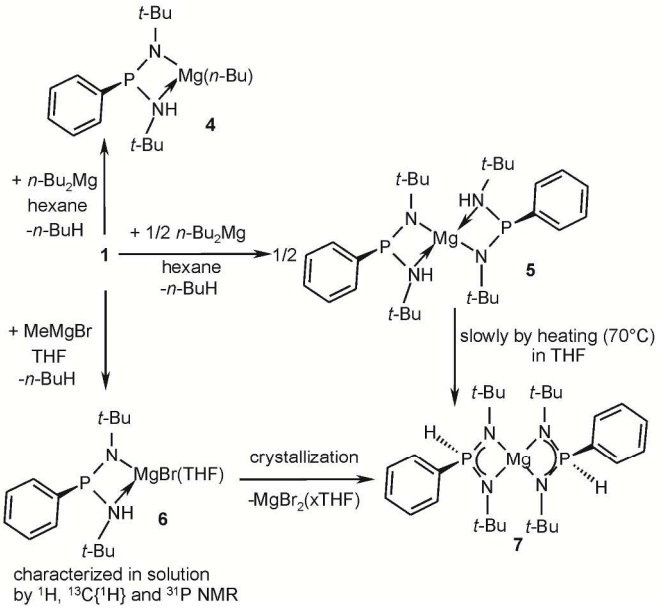

Scheme 2 Reactivity of **1** with *n*-Bu_2Mg and MeMgBr.

Analogously, heating of a THF solution of **5** (70°C) led to magnesium phosphinate $[Ph(H)P(Nt\text{-}Bu)_2]_2Mg$ (7) (Scheme 1) as monitored and judged by the ^1H and ^{31}P NMR spectroscopy. However, this tautomeric shift is significantly slower than in the case of the aluminum derivative (less than 10% conversion after 5 days) and more importantly prolonged heating of **5** resulted in the formation of numerous side-products. Nevertheless, the phosphinate **7** is easily accessible by the treatment of **1** with MeMgBr (Scheme 2). In the first step of this reaction, compound [PhP(NH*t*-Bu)(N*t*-Bu)]MgBr(THF) (**6**) is formed as shown by the analysis of the evaporated reaction mixture by ^1H, $^{13}C\{^1H\}$ and ^{31}P NMR spectroscopy. Thus, ^1H and $^{13}C\{^1H\}$ NMR spectra proved the presence of two magnetically non-equivalent *t*-Bu groups [$\delta(^1H)$ = 1.34 and 1.57 ppm; $\delta(^{13}C$, for $C(CH_3))$ = 31.2 and 35.9 ppm] and the N*H* group [$\delta(^1H)$ = 1.80 ppm]. Furthermore, the signals due to the coordinated THF were detected as well [$\delta(^1H)$ = 1.14 and 3.55 ppm; $\delta(^{13}C)$ = 25.3 and 69.7 ppm]. The ^{31}P NMR spectrum of **6** revealed one singlet at 89.1 ppm close to the values observed for related **4** and **5**. Interestingly, all attempts for re-crystallization of **6** to obtain an analytically pure sample resulted in both elimination of magnesium bromide and tautomeric hydrogen shift giving phosphinate **7** (Scheme 2). This procedure is also applicable on a preparative-scale (yield of **7** after recrystallization is 64 %). Compound **7** was isolated as colourless crystals well soluble in aromatic solvents. The ^1H and ^{13}C NMR spectra revealed expected set of signals. The

observation of doublets at 7.76 ppm in the ^{1}H NMR spectrum and at 8.9 ppm ($^1J_{P-H}$ = 432 Hz) in the ^{31}P NMR spectrum proved formation of the *PH* functionality and thereby the tautomeric shift. These values are also well comparable to related aluminum phosphinates reported by us earlier.[7]

The reaction of **2** with 1 molar equivalent of *n*-Bu_2Mg in THF gave compound $\{[PhP(NPh)_2]_2Mg(THF)_2\}_2$ (**8**) as the result of deprotonation of both NH functionalities (Scheme 3). This finding is in contrast to the phosphane **1**, where the deprotonation of the second NH group was not possible (Scheme 2). Importantly, all attempts to obtain a heteroleptic compound (similar to **4**) remained unsuccessful probably reflecting higher acidity of the N*H* group of **2** in comparison with **1**. Compound **8** crystallized in the form of colourless single-crystals from benzene and is nearly insoluble in THF and aliphatic solvents. The ^{1}H and ^{13}C{^{1}H} NMR spectra revealed one set of expected signals for the phenyl substituents and coordinated THF molecules [$\delta(^1H)$ = 1.10 and 3.31 ppm; $\delta(^{13}C)$ = 25.5 and 69.8 ppm]. The ^{31}P NMR spectrum contained one singlet at 93.3 ppm [$\delta(^{31}P)$ = 46.8 ppm for the parent phosphane **2**]. Importantly, there was no evidence for the presence of the N*H* group thereby proving full deprotonation of the bis(amino)phosphane **2**.

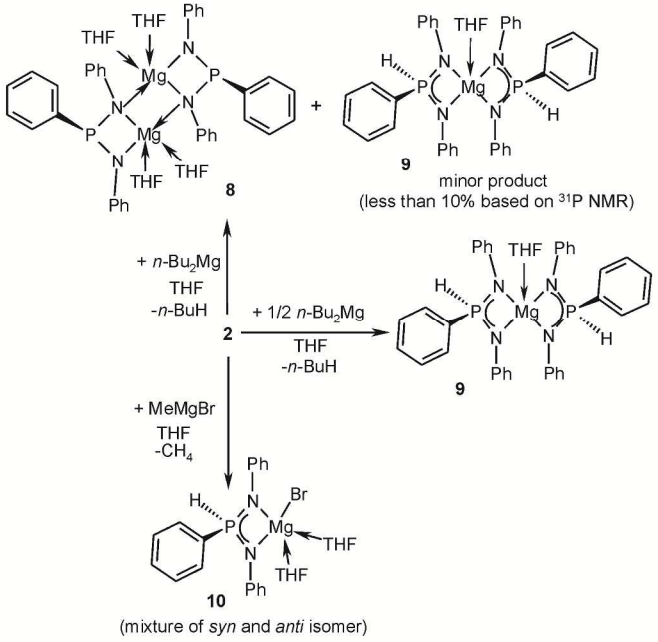

Scheme 3 Reactivity of **2** with *n*-Bu_2Mg and MeMgBr.

Importantly, crude reaction mixtures during preparation of **8** were always contaminated by a remarkable (10-15%) amount of a by-product, which was shown to be the phosphinate $[Ph(H)P(NPh)_2]_2Mg(THF)$ (**9**). This compound may be isolated from this mixture, but it is better prepared (in yield of 42 %) by the reaction of **2** with 0.5 molar equivalent of *n*-Bu_2Mg (Scheme 3). Compound **9** was isolated as colourless crystals soluble in aromatic solvents and moderately in THF. The ^{1}H and ^{31}P NMR spectra revealed doublets [at $\delta(^1H)$ = 8.31 ppm; $\delta(^{31}P)$ = 11.6 ppm; $^1J_{P-H}$ = 442 Hz] confirming the presence of the *PH* group and the tautomerization leading to the phosphinate backbone. The ^{1}H and ^{13}C{^{1}H} NMR spectra contained one set of expected signals for the phenyl substituents and coordinated THF molecule [$\delta(^1H)$ = 1.27 and 3.63 ppm; $\delta(^{13}C)$ = 25.8 and 68.9 ppm]. The treatment of **2** with MeMgBr (Scheme 2) resulted in the formation of the phosphinate $[Ph(H)P(NPh)_2]MgBr(THF)_2$ (**10**) and methane elimination. Compound **10** was obtained as colourless crystals well soluble in THF and aromatic solvents. It is also noteworthy that compound **10** is the PH tautomeric form. Similar reaction of the phosphane **1** with MeMgBr, gave compound **6**, which represents the NH tautomer. This fact is reflected in different behaviour of both compounds. While compound **6** was seen only as an intermediate in the formation of the final product **7**, the phosphinate **10** is fairly stable and showed no tendency for any elimination of magnesium bromide. This finding well coincides with our recent findings (including a theoretical approach), which showed that derivatives of the phosphane **2** are more liable to the NH→PH tautomeric transformation in comparison with **1**.[7] This tautomerization and formation of the phosphinate backbone is also most probably responsible for higher stability of **10** compared to **6**. The ^{31}P NMR spectra of **10** (both of isolated single-crystals and bulk sample, in THF-d8) surprisingly revealed two doublets [$\delta(^{31}P)$ = 8.9 ppm; $^1J_{P-H}$ = 439.9 Hz and $\delta(^{31}P)$ = 9.3 ppm; $^1J_{P-H}$ = 444.3 Hz] similarly two doublets were detected in corresponding ^{1}H NMR spectrum indicating the presence of two species containing *PH* functionality [$\delta(^1H)$ = 8.16 ppm; $^1J_{P-H}$ = 439.9 Hz and $\delta(^{31}P)$ = 8.27 ppm; $^1J_{P-H}$ = 444.3 Hz]. The integral ratio between both species is 1:0.85. Analogously, two sets of signals were observed for remaining atoms in ^{1}H and ^{13}C{^{1}H} NMR spectra. The observation of these two species is most probably caused by the presence of different isomers of **10** in solution. To approve this hypothesis, the ^{31}P-^{31}P EXSY NMR spectrum of **10** in THF-d8 was acquired. Appropriate cross-peaks were observed for two isomers of compound **10** (mixing time being from 0.1 to 1.5 s, Figure 3) indicating that isomers are in a slow chemical exchange on the NMR time scale.

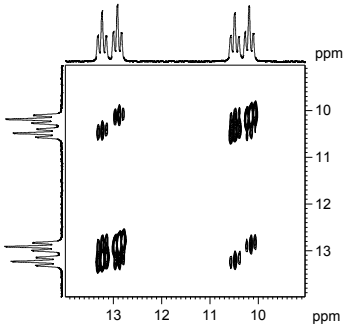

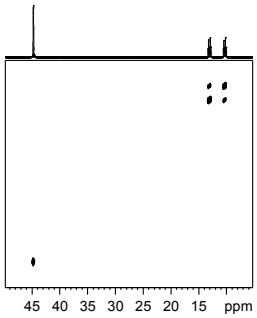

Figure 3 ^{31}P-^{31}P EXSY NMR spectrum of **10** (top) and ^{31}P-^{31}P EXSY NMR spectrum of **10** in the mixture with free ligand (bottom) in THF-d8, mixing time 1s.

We added some an amount of the parent phosphane **2** to the solution of compound **10** and repeated ^{31}P-^{31}P EXSY measurement (mixing time being again from 0.1 to 1.5 s, Figure 3). No additional cross-peaks were observed and, thus, no exchange exists for the free phosphane and any isomer of compound **10** under above mentioned experimental conditions. Isomers of **10** are probably formed by different orientations of the phosphorus bonded phenyl ring and the bromine atom attached to the central planar $MgPN_2$ core (Figure 4). Thus, two possible isomers came into mind. It is the *syn*-**10** (also observed in the solid state *vide infra*) and *anti*-**10**. A third isomer with the bromine atom in the same plane as the MgN_2P core (isomer *plane*-**10**) is also considered (Figure 4). To shed more light to this phenomenon, a theoretical survey dealing with suggested isomers of **10** was performed.

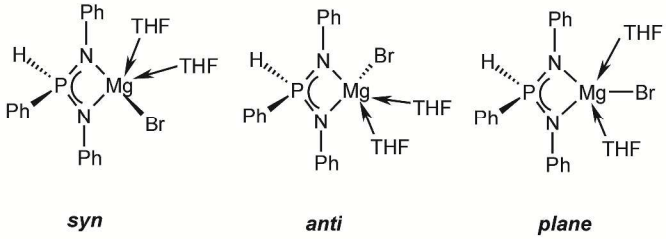

Figure 4 Schematic drawing of anticipated isomers of **10**.

First, the performance of different DFT methods (BP86-D, M06 and B3LYP-D) in reproducing the molecular structure of the *syn*-**10** isomer was assessed by the comparison with the X-ray diffraction data. Several statistical criteria were considered in our benchmark study: the root-mean-square deviation (RMSD) between the DFT/cc-pVDZ-optimized and X-ray set of Cartesian coordinates and the mean absolute error (MAE) from comparison of selected interatomic distances and dihedral angles. Table 1 contains the RMSD for the superimposed structures (Figure 5) considering the geometry of the $MgPN_2$ core alone ($RMSD_4$) and all atoms ($RMSD_{65}$) together with the MAE for the bond lengths and dihedral angles. The M06-optimized geometry is in better agreement with the X-ray structure when considering the overall structure. However, The lowest $RMSD_4$ and $MAE_{torsions}$ correspond to the B3LYP-D geometries. In any case, the optimized geometries obtained with B3LYP-D and M06 are very similar according to the RMSD and MAE values. On the other hand, BP86 gives the largest statistical errors. Moreover, extending the basis set to the aug-cc-pVDZ is seen to improve the optimized structures (Figure 5), as the RMSD and MAE values are significantly reduced. Therefore, the B3LYP-D/aug-cc-pVTZ level of theory was chosen to perform the optimization and frequency calculations of the *syn*- and *anti*- isomers of **10**.

Table 1. Root mean square deviations (RMSD in Å) and mean absolute errors (MAE) of the DFT optimized geometries relative to the X-ray structures of the *syn*-**10** isomer together with the relative energies of different isomers (E in kcal mol^{-1}).[a]

method	$RMSD_4$	$RMSD_{65}$	MAE_{bonds}	$MAE_{torsions}$	*syn***10**	*anti***10**	*plane***10**
BP86-D[b]	0.038	0.470	0.082	4.64	0.00	0.47	2.11
M06[b]	0.034	0.410	0.073	4.21	0.00	2.04	3.89
B3LYP-D[b]	0.029	0.424	0.074	4.01	0.00	1.27	3.24
B3LYP-D[c]	0.029	0.382	0.073	3.45	0.00	1.70	3.34

[a] *Zero-point corrected relative energies.* [b] *The cc-pVDZ basis set was used for the optimization and frequency calculations.* [c] *The aug-cc-pVDZ basis set was used.*

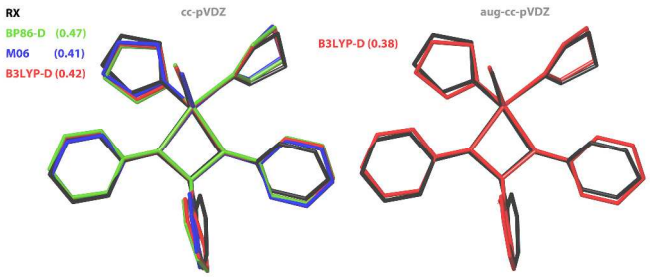

Figure 5. Comparison of BP86-D, B3LYP-D and M06-optimized geometries of *syn*-**10** isomer, overlaid with the X-ray structure. The all-atom RMSDs (in Å) are also displayed.

The zero-point corrected relative energies of the *syn*-, *anti*- and *plane*- isomers of **10** computed with the different functionals are collected in Table 1. Importantly, all the methods predict that the *syn*- isomer is the most stable, followed by the *anti*-isomer. The small energy difference between the *syn*- and *anti*-isomers computed with all the methods suggests that both isomers coexist in a dynamic equilibrium in solution of **10**. The *plane*- isomer is less stable, being more than 3 kcal mol^{-1} higher in energy than the *syn*- conformer according to B3LYP-D and M06 energies. Moreover, the use of diffuse basis functions does not change significantly the relative energies of the different isomers of **10**.

Table 2. Relative energies (E), enthalpies (ΔH) and Gibbs free energies (ΔG) for the different isomers of **10** (in kcal mol^{-1}) in gas phase and different solvents computed at the B3LYP-D/aug-cc-pVTZ level of theory.[a]

method	E_{gas}	ΔH_{gas}	ΔG_{gas}	E_{bz}	ΔH_{bz}	E_{THF}	ΔH_{THF}
syn-**10**	0.00	0.00	0.00	0.00	0.00	0.00	0.00
anti-**10**	1.21	1.34	3.14	1.72	2.06	2.04	2.20
plane-**10**	3.49	3.30	2.70	2.38	2.52	2.56	2.33

[a] *Thermochemical corrections computed at the B3LYP/aug-cc-pVDZ level of theory at 298.15 K and 1 atm.*

Increasing to a triple ζ-basis set results in an electronic energy difference of 1.2 kcal mol^{-1} between the *syn*- and the *anti*-conformations. Inclusion of the thermochemical corrections yields a relative enthalpy of 1.35 kcal mol^{-1} and a relative Gibbs free energy of 3.13 kcal mol^{-1} for the *syn*- isomer. In addition, solvation energies in benzene and THF were calculated by using the SMD model (Table 2). In both solvents, the *syn*-isomer of **10** is predicted to be the most stable conformation. Nevertheless, the energy difference between the *syn*- and *anti*-isomers increases as the dielectric constant increases, whereas the *plane*- isomer becomes more stable. All these findings indicate that compound **10** exist in solution as a mixture of two isomers *syn*-**10** and *anti*-**10,** while the presence of *plane*-**10** seems to be less probable.

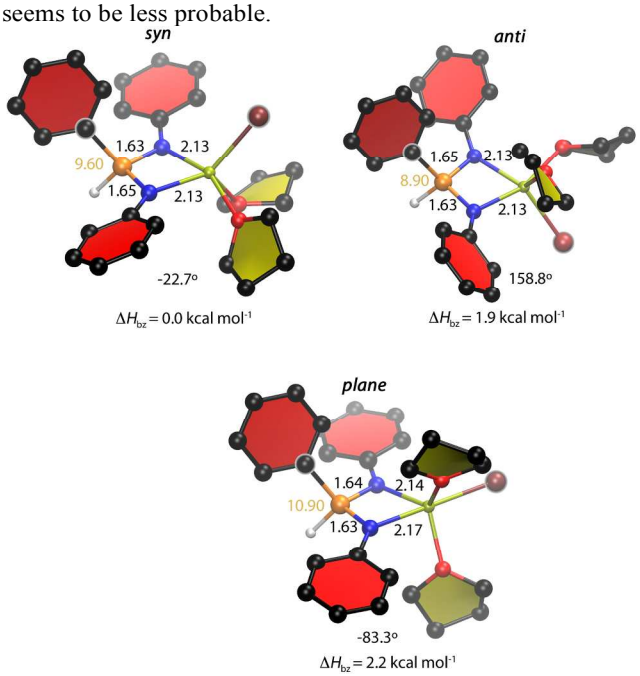

Figure 6. B3LYP-D/aug-cc-pVDZ optimized geometries of the *syn*-, *anti*- and *plane*- isomers of **10**. The Mg-N and P-N distances (in Å), Br-Mg-P-C dihedral angle (in °) and relative enthalpies in benzene (in kcal mol^{-1}) are also displayed. The computed δ(^{31}P) (in ppm) are shown in orange.

Finally, the ^{31}P chemical shifts for the three isomers were computed using the GIAO/B3LYP/cc-pVTZ method. Interestingly, the computed δ(^{31}P) of the *syn*- and *anti*- isomers are in excellent agreement with the experimental chemical shifts (9.3 and 8.9 ppm), providing an additional evidence for the presence of both isomers in solution of **10.** On the other hand, the computed δ(^{31}P) of the *plane* isomer is deshielded by 1.6 ppm compared to the experimental values found for both isomers.

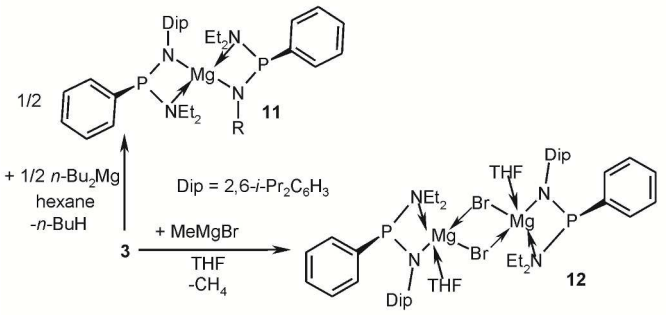

Scheme 4 Reactivity of **3** with *n*-Bu_2Mg and MeMgBr.

Finally, the reactivity of potentially monoanionic phosphane **3** was studied for comparison as in this case no tautomerization is possible. Thus, the reaction between **3** and *n*-Bu_2Mg in 1:0.5 molar ratio in hexane smoothly gave $[PhP(NEt_2)(NDip)]_2Mg$ (**11**) (in yield of 49 %) as colourless crystals soluble in aromatic and moderately in aliphatic solvents. The ^{31}P NMR spectrum of **11** revealed one signal at 122.1 ppm significantly shifted in comparison with the value found for the starting phosphane **3** [δ(^{31}P) = 82.5 ppm]. The ^{1}H and ^{13}C{^{1}H} NMR spectra of **3** revealed one set of relatively broad signals for both *Dip*N a N*Et*$_2$ groups. The treatment of **3** with one molar equivalent of MeMgBr (Scheme 3) in THF produced compound $\{[PhP(NEt_2)(NDip)_2]Mg(\mu\text{-}Br)(THF)\}_2$ (**12**) in 69% yield as a colourless solid soluble in aromatic solvents and THF. The ^{31}P NMR spectrum of **12** revealed one signal at 127.6 ppm close to the value found for **11**. The ^{1}H and ^{13}C{^{1}H} NMR spectra of **12** revealed signals of coordinated THF [δ(^{1}H) = 1.07 and 3.57 ppm; δ(^{13}C) = 25.2 and 70.5 ppm] and one set of relatively broad signals for both *Dip*N a N*Et*$_2$ groups.

Solid state structures

The molecular structures of **5**, **7-12** were determined using single-crystal X-ray diffraction analysis (Figures 7-14) and the crystallographic data are summarized in the Experimental section.

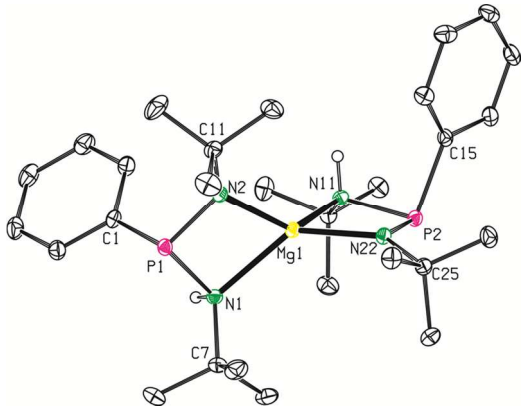

Figure 7 Molecular structure of **5** (40% probability displacement ellipsoids). Hydrogen atoms except of NH groups are omitted for clarity. Selected bond lengths [Å] and bonding angles [deg]: Mg(1)-N(1) 2.2079(15), Mg(1)-N(11) 2.1835(15), Mg(1)-N(2) 1.9864(18), Mg(1)-N(22) 1.9879(15), P(1)-N(1) 1.8047(18), P(1)-N(2) 1.6590(15), P(2)-N(11) 1.7983(14), P(2)-N(22) 1.6724(14), N(1)-Mg(1)-N(11) 117.39(6), N(2)-Mg(1)-N(22) 133.36(7), N(1)-Mg(1)-N(22) 135.87(7), N(2)-Mg(1)-N(11) 129.85(7), N(1)-Mg(1)-N(2) 74.30(7), N(11)-Mg(1)-N(22) 74.33(5), N(1)-P(1)-N(2) 94.19(8), N(11)-P(2)-N(22) 93.27(7).

The Mg(1) atom in **5** is four-coordinated and adopts a distorted tetrahedral coordination environment (Figure 7). The Mg(1)-N(2) and Mg(1)-N(22) bond lengths of 1.9864(18) and 1.9879(15) Å, respectively, are slightly shorter than the Σ_{cov}(N, Mg) = 2.10 Å.[13] In contrast, the Mg(1)-N(1) and Mg(1)-N(11) bond lengths [2.2079(15) and 2.1835(15) Å] are longer and indicate the presence of strong N→Mg intramolecular interaction rather than a covalent bond. This fact is further reflected by the geometry around respective nitrogen atoms, which is essentially trigonal planar for N(2) and N(22), while it is tetrahedral in the case of NH groups [N(1) and N(11) atoms]. Similar difference is also observed for P-N bonds, because P(1)-N(2) and P(2)-N(22) bond lengths [1.6590(15) and 1.6722(14) Å] are significantly shorter than P(1)-N(1) and P(1)-N(11) [1.8047(18) and 1.7983(14) Å]. The latter values coincide with the theoretical single bond Σ_{cov}(N, P) = 1.82 Å[13], while the former correspond better to the double bond Σ_{cov}(N, P) = 1.62 Å.[13] Similarly coordinated magnesium amide has recently been reported by Chivers *et al.* [$(Me_3SiN{=})P(NH$*t*$-Bu)_2(N$*t*$-Bu)]_2Mg$, but this compound is in its behavior a phoshinate rather than phosphane.[9b]

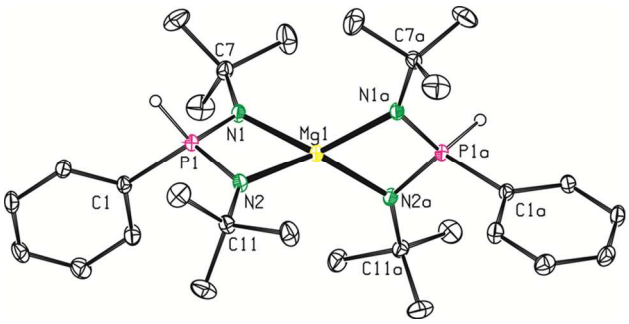

Figure 8 Molecular structure of **7** (40% probability displacement ellipsoids). Hydrogen atoms except of PH groups are omitted for clarity. The symmetry operator a = -x, y, ½-z. Selected bond lengths [Å] and bonding angles [deg]: Mg(1)-N(1) 2.0546(13), Mg(1)-N(2) 2.0453(18), P(1)-N(1) 1.597(2), P(1)-N(2) 1.5989(15), N(1)-Mg(1)-N(2) 73.55(7), N(1)-Mg(1)-N(1a) 129.53(7), N(1)-Mg(1)-N(2a) 127.65(8), N(2)-Mg(1)-N(2a) 134.79(7), N(2)-Mg(1)-N(1a) 127.65(8), N(1)-P(1)-N(2) 100.37(8).

Compound **7** crystallized in the centrosymmetric C2/c space group and its molecular structure proved the presence of PH group and the formation of a phosphinate backbone (Figure 8). The central Mg(1) atom is tetrahedraly coordinated. In contrast to **5**, the Mg(1)-N(1) and Mg(1)-N(2) bond lengths of 2.0546(13) and 2.0453(18) Å, respectively, are nearly identical and correspond to the Σ_{cov}(N, Mg) = 2.10 Å.[13] Analogously, the P(1)-N(1) and P(1)-N(2) distances [1.597(2) and 1.5989(15) Å] are very similar suggesting effective delocalization of the negative charge across the NPN phosphinate backbone and its symmetrical bonding to the central Mg(1) atom. The N(1)-P(1)-N(2) bonding angle of 100.37(8)° is wider than the corresponding angle in **5** [94.19(8) and 93.27(7)°], while the N(1)-Mg(1)-N(2) bonding angle 73.55(7)° is comparable with the corresponding values in **5** [74.30(7) and 74.33(5)°]. The main structural parameters of **7** resemble those found for the phosphinate $[Ph_2P(NSiMe_3)_2]_2Mg$[9a] [for example the Mg-N bonds in the latter fall into the interval 2.068(2)-2.083(2) Å], but small difference may be found in the N-P-N bonding angle, which is more acute in **7**. This marginal feature may be ascribed to a different substitution on both P and N atoms in **7** and $[Ph_2P(NSiMe_3)_2]_2Mg$.[9a]

Compound **8** forms a centrosymmetric dimer in the solid state (Figure 9) *via* two strong intermolecular contacts with the distances Mg(1)-N(1a) and Mg(1a)-N(1) of 2.1409(14) Å approaching Σ_{cov}(N, Mg) = 2.10 Å.[13] The central Mg(1) atom is coordinated by the ligand in a non-symmetric fashion as demonstrated by fairly different distances Mg(1)-N(1) 2.2978(16) Å *vs.* Mg(1)-N(2) 2.0680(15) Å. This fact is also reflected in slightly different P(1)-N(1) and P(1)-N(2) bond lengths of 1.7241(14) and 1.6985(15) Å, respectively. The coordination sphere of the Mg(1) atom is further saturated by two THF molecules [Mg(1)-O(1) 2.0852(12) and Mg(1)-O(2) 2.1346(14) Å; Σ_{cov}(O, Mg) = 1.99 Å[13]]. The Mg(1) atom is, thus, five-coordinated and resulting polyhedron may be described as an intermediate between the square pyramid and the trigonal bipyramid with the τ value of 0.65.[14] All three four-membered Mg_2N_2 and MgN_2P rings are essentially planar and share their edges with formation of a ladder-like structure. Similar structural motif with three mutually connected four-membered rings was determined for the magnesium amidinate $\{[MeC(NEt)(N$*t*$-Bu)]_2Mg\}_2$ by Winter *et al.*[15]

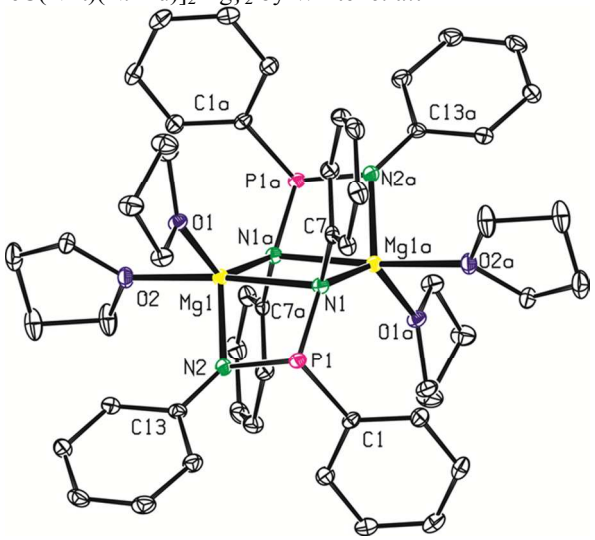

Figure 9 Molecular structure of **8** (40% probability displacement ellipsoids). Hydrogen atoms and benzene solvent molecule are omitted for clarity. The symmetry operator a = 1-x, 1-y, -z. Selected bond lengths [Å] and bonding angles [deg]: Mg(1)-N(1) 2.2978(16), Mg(1)-N(2) 2.0680(15), Mg(1)-N(1a) 2.1409(14), Mg(1)-O(1) 2.0852(12), Mg(1)-O(2) 2.1346(14), P(1)-N(1) 1.7241(14), P(1)-N(2)

1.6985(15), N(1)-Mg(1)-N(2) 72.06(5), N(1)-Mg(1)-O(1) 93.40(5), N(1)-Mg(1)-O(2) 175.18(5), N(1)-Mg(1)-N(1a) 87.73(5), N(2)-Mg(1)-O(1) 98.31(5), N(2)-Mg(1)-O(2) 103.12(6), N(2)-Mg(1)-N(1a) 123.46(6), O(1)-Mg(1)-O(2) 87.38(5), O(1)-Mg(1)-N(1a) 136.05(5), O(2)-Mg(1)-N(1a) 95.01(6), Mg(1)-N(1)-Mg(1a) 92.27(6), N(1)-P(1)-N(2) 97.58(7).

Although compound **8** crystalizes as a dimer from benzene (vide supra), occasionally single-crystals were also obtained from a saturated THF solution and showed a monomeric structure (**8a**, Figure 10). The unit cell of **8a** contains two independent molecules, but they are closely structurally related and only one of them is discussed here in detail. The central Mg(1) atom is five-coordinated in **8a** by the ligand and three oxygen atoms coming from coordinated THF molecules [Mg(1)-O(1) 2.035(4), Mg(1)-O(2) 2.053(3) and Mg(1)-O(3) 2.104(4) Å; Σ_{cov}(O, Mg) = 1.99 Å[13]]. The Mg(1)-N(1) and Mg(1)-N(2) [2.048(4) and 2.058(4) Å] as well as P(1)-N(1) and P(1)-N(2) [1.699(4) and 1.703(4) Å] bond lengths are nearly identical and slightly shorter than values expected for single bonds [Σ_{cov}(N, P) = 1.82 Å and Σ_{cov}(N, Mg) = 2.10 Å].[13] The central MgN_2P is again essentially planar. The coordination polyhedron of the central atom is again strongly distorted, but closer to the square pyramid than to the trigonal bipyramid as indicated by the value $\tau = 0.30$.[14] Chivers *et al.* reported on an analogous monomeric four-membered ring compound stabilized by a boramidinate ligand $PhB(NDip)_2Mg(THF)_2$,[16] but in this case the central atom is only four-coordinated and adopts a tetrahedral shape. Similarly, compound $Ph_2Si(NDip)_2Mg(THF)_2$ contains a four-membered ring system.[17] The presence of bulky Dip groups in the later compounds is most probably responsible for the coordination of only two THF molecules in contrast to **8a**, where three THF donors are present.

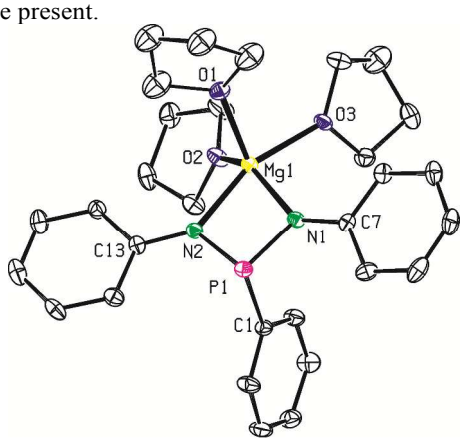

Figure 10 Molecular structure of **8a** (40% probability displacement ellipsoids, only one of two independent molecules in the unit cell and only one position of disordered C(19) and C(22) is shown). Hydrogen atoms and THF solvent molecule are omitted for clarity. Selected bond lengths [Å] and bonding angles [deg]: Mg(1)-N(1) 2.046(6), Mg(1)-N(2) 2.061(6), Mg(1)-O(1) 2.034(5), Mg(1)-O(2) 2.055(5), Mg(1)-O(3) 2.104(5), P(1)-N(1) 1.701(6), P(1)-N(2) 1.703(5), N(1)-Mg(1)-N(2) 73.1(2), N(1)-Mg(1)-O(1) 116.0(2), N(1)-Mg(1)-O(2) 141.9(2), N(1)-Mg(1)-O(3) 94.4(2), N(2)-Mg(1)-O(1) 107.0(2), N(2)-Mg(1)-O(2) 95.3(2), N(2)-Mg(1)-O(3) 160.1(2), O(1)-Mg(1)-O(2) 102.1(2), O(1)-Mg(1)-O(3) 92.3(2), O(2)-Mg(1)-O(3) 85.0(2), N(1)-P(1)-N(2) 91.90(3).

Phosphinate **9** (Figure 11) is formally an analogue of compound **7**, but the presence of less stericaly demanding phenyl groups instead of *t*-Bu moieties in **7** most probably allows increasing of the coordination number of the central Mg(1) atom by accommodation of an additional THF molecule in its coordination sphere [Mg(1)-O(1) 2.059(2) Å]. The coordination polyhedron is again found on the border between the square pyramid and the trigonal bipyramid (τ = 0.68[14]). The coordination of the NPN phosphinate anion to the Mg(1) atom is symmetrical as indicated by the Mg-N bond lengths found in a narrow interval 2.114(2)-2.124(2) Å, but these values are slightly longer than those obtained for **7**. The P-N bond lengths in **9** fall into the interval 1.598(2)-1.608(2) Å.

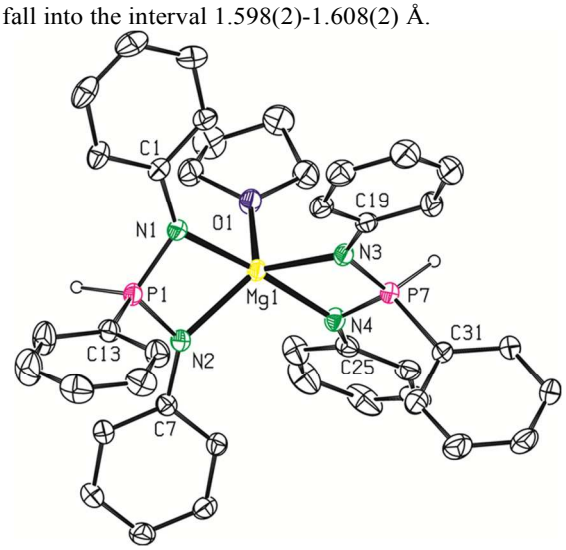

Figure 11 Molecular structure of **9** (40% probability displacement ellipsoids). Hydrogen atoms except PH groups and THF and toluene solvent molecules are omitted for clarity. Selected bond lengths [Å] and bonding angles [deg]: Mg(1)-N(1) 2.1214(19), Mg(1)-N(2) 2.123(2), Mg(1)-N(3) 2.113(2), Mg(1)-N(4) 2.1239(19), Mg(1)-O(1) 2.057(2), P(1)-N(1) 1.599(2), P(1)-N(2) 1.6070(19), P(7)-N(3) 1.6072(19), P(7)-N(4) 1.605(2), N(1)-Mg(1)-N(2) 70.43(8), N(1)-Mg(1)-N(3) 108.89(8), N(1)-Mg(1)-N(4) 174.03(9), N(1)-Mg(1)-O(1) 93.24(8), N(2)-Mg(1)-N(3) 133.45(9), N(2)-Mg(1)-N(4) 105.29(8), N(2)-Mg(1)-O(1) 117.43(8), N(3)-Mg(1)-N(4) 70.76(8), N(3)-Mg(1)-O(1) 109.14(8), N(4)-Mg(1)-O(1) 92.47(8), N(1)-P(1)-N(2) 99.51(10), N(3)-P(7)-N(4) 99.56(10).

Compound **10** exists in solution as two isomers that are in a dynamic equilibrium (*anti*-**10** and *syn*-**10**, vide supra) and from this solution single-crystals of *syn*-**10** were obtained preferably in all cases and its structure is shown in Figure 12. The central MgN_2P core remains essentially planar and the phenyl group and the bromine atom are located in *syn* fashion. The Mg(1)-N(1) and Mg(1)-N(2) bond lengths [2.150(2) and 2.087(3) Å] are mutually a bit more different in comparison with phosphinates **7** and **9**. Nevertheless, the P(1)-N(1) and P(1)-N(2) distances [1.606(2) and 1.602(2) Å] within the phosphinate backbone are essentially identical and also the N(1)-P(1)-N(2) bonding angle [98.86(12)°] resembles those established for **7** and **9**. The Mg(1)-Br(1) bond length of 2.4917(12) Å corresponds to the Σ_{cov}(Br, Mg) = 2.53 Å.[13] The central Mg(1) atom is further coordinated by two THF molecules [Mg(1)-O(1) 2.061(2) and Mg(1)-O(2) 2.115(2) Å; Σ_{cov}(O, Mg) = 1.99 Å[13]]. The value τ of 0.48[14] for *syn*-**10**

indicates an intermediate coordination geometry around Mg(1) atom between the square pyramid and the trigonal bipyramid. *Syn*-**10** is rare example of a heteroleptic magnesium(II) phosphinate. To the best of our knowledge, the only analogues $Ph_2P(NDip)_2MgX(Et_2O)$ (where X = Br or I) have recently been synthesized by Stasch.[10] Nevertheless, there is a number of related magnesium amidinates: for example $RC(NR')_2MgX(L)$ (R = CCPh, PPh_2, PCy_2; R′ = *i*-Pr, Cy; X = Cl, Br; L = THF, Et_2O) have recently been characterized.[18]

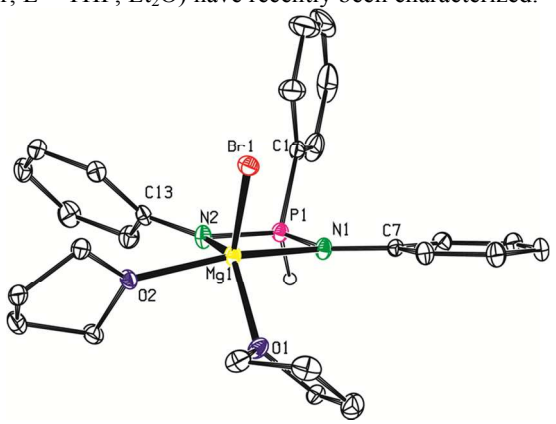

Figure 12 Molecular structure of *syn*-**10** (40% probability displacement ellipsoids). Hydrogen atoms except of PH groups are omitted for clarity. Selected bond lengths [Å] and bonding angles [deg]: Mg(1)-N(1) 2.150(2), Mg(1)-N(2) 2.087(3), Mg(1)-Br(1) 2.4917(12), Mg(1)-O(1) 2.061(2), Mg(1)-O(2) 2.115(2), P(1)-N(1) 1.606(2), P(1)-N(2) 1.602(2), N(1)-Mg(1)-N(2) 70.21(9), N(1)-Mg(1)-Br(1) 105.83(8), N(1)-Mg(1)-O(1) 96.14(8), N(1)-Mg(1)-O(2) 156.63(11), N(2)-Mg(1)-Br(1) 126.06(7), N(2)-Mg(1)-O(1) 128.08(10), N(2)-Mg(1)-O(2) 90.07(10), Br(1)-Mg(1)-O(1) 105.84(8), Br(1)-Mg(1)-O(2) 95.81(7), O(1)-Mg(1)-O(2) 86.11(8), N(1)-P(1)-N(2) 98.86(12).

Molecular structure of **11** is shown in Figure 13 and is structurally related to **5**. The central Mg(1) atom is tetrahedraly coordinated by two chelating phosphanes. The Mg(1)-N(1) and Mg(1)-N(3) bond lengths [2.0026(13) and 2.0220(14) Å] are shorter in comparison with Mg(1)-N(2) and Mg(1)-N(4) distances [2.2262(14) and 2.1796(14) Å] indicating the presence of a strong $Et_2N\rightarrow Mg$ intramolecular interaction rather than a covalent bond in the latter case (compare with the Σ_{cov}(N, Mg) = 2.10 Å[13]). Analogously, the P(1)-N(2) and P(2)-N(4) distances [1.8443(13) and 1.8399(14) Å] are significantly elongated in comparison with the P(1)-N(1) and P(2)-N(3) bonds [1.6648(13) and 1.6756(13) Å]. The latter values coincide with the double bond Σ_{cov}(N, P) = 1.62 Å[13], while the former correspond better to the single bond Σ_{cov}(N, P) = 1.82 Å.[13] The N(1)-P(1)-N(2) and N(3)-P(1)-N(4) bonding angles of 93.45(6) and 93.77(6)°, respectively, well correspond to the values found in **5**.

The unit cell of **12** contains two independent molecules, but they are closely structurally related and only one of them is discussed here in detail. Compound **12** forms a dimer in the solid state *via* two non-symmetrical μ-bromo- bridges (Figure 14), where the Mg(1)-Br(1) and Mg(1)-Br(1a) bond lengths are 2.5773(8) and 2.7089 Å, respectively (compare with the Σ_{cov}(Br, Mg) = 2.53 Å[13]). The coordination polyhedron of the central metal, which is completed by two nitrogen and oxygen atom from coordinated THF molecule [Mg(1)-O(1) 2.0409(19) Å], is with the τ value of 0.66 between the square pyramid and the trigonal bipyramid similarly to **8**. The Mg(1)-N(1) and Mg(1)-N(2) bond lengths [2.010(4) and 2.296(2) Å] are comparable to the values observed in **11** and analogously P(1)-N(1) and P(1)-N(2) bond lengths [1.671(2) and 1.811(2) Å] are similar to **11**. All three four-membered rings in **12** are planar. Similar dimers formed *via* halogen bridges are known for magnesium amidinates and guanidates such as $[Ph_2PC(NCy)_2Mg(THF)(\mu\text{-}Cl)]_2$[18] or $[i\text{-}Pr_2NC(NDip)_2Mg(THF)(\mu\text{-}I)]_2$.[19]

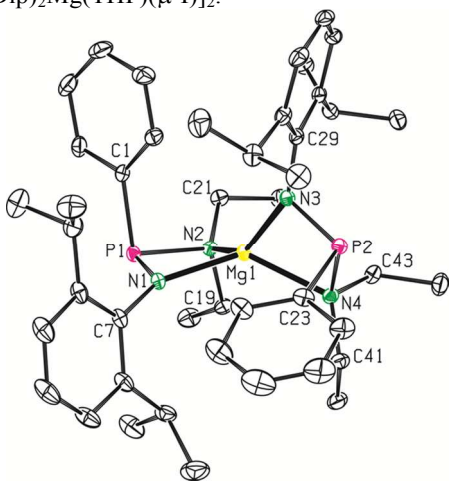

Figure 13 Molecular structure of **11** (40% probability displacement ellipsoids). Hydrogen atoms are omitted for clarity. Selected bond lengths [Å] and bonding angles [deg]: Mg(1)-N(1) 2.0026(13), Mg(1)-N(2) 2.2262(14), Mg(1)-N(3) 2.0220(14), Mg(1)-N(4) 2.1796(14), P(1)-N(1) 1.6648(13), P(1)-N(2) 1.8443(13), P(2)-N(3) 1.6756(13), P(2)-N(4) 1.8399(14), N(1)-Mg(1)-N(2) 74.23(5), N(1)-Mg(1)-N(3) 128.84(5), N(1)-Mg(1)-N(4) 133.88(6), N(2)-Mg(1)-N(3) 136.25(5), N(2)-Mg(1)-N(4) 117.95(5), N(3)-Mg(1)-N(4) 75.27(5), N(1)-P(1)-N(2) 93.45(6), N(3)-P(2)-N(4) 93.77(6).

To summarize, it is evident from the determined molecular structures of **5**, **7**-**12** that the tautomeric NH→PH shift with the formation of a phosphinate backbone is reflected also in the main structural features of these complexes. Thus, the coordination of the NPN backbone to the central magnesium atom in phosphinates **7**, **9** and *syn*-**10** is essentially symmetrical regarding both Mg-N and P-N bonds pointing to a delocalization of the negative charge over this system. In contrast, there is a significant difference between respective Mg-N and P-N bonds found in amino-amidophosphanes **5**, **11** and **12**. Bis(amido)phosphanes **8** and **8a** represent special cases, in the first one the NPN core is strongly distorted by the formation of an intermolecular contact. The ligand in **8a** exhibits symmetrical coordination similarly to phosphinates **7**, **9** and *syn*-**10**, but P-N bond distances in **8a** are elongated about 0.1 Å in comparison with **7**, **9** and *syn*-**10**. There is also significant difference in the value of N-P-N bonding angles. This value falls into the interval 91.90(17)-94.98(10)° in **5**, **8a**, **11** and **12**, while wider angles were observed in phosphinates **7**, **9** and *syn*-**10** [98.86(12)-100.37(8)°]. The presence of the lone pair at the phosphorus atom in **5**, **8a**, **11** and **12** is most probably responsible for this deviation as the phosphorus atom

in phosphinates lacks it. In contrast, the N-Mg-N bonding angles lie in a narrow interval 70.21(9) (*syn*-**10**)-75.27(5)° (**11**) with no obvious trend among studied complexes.

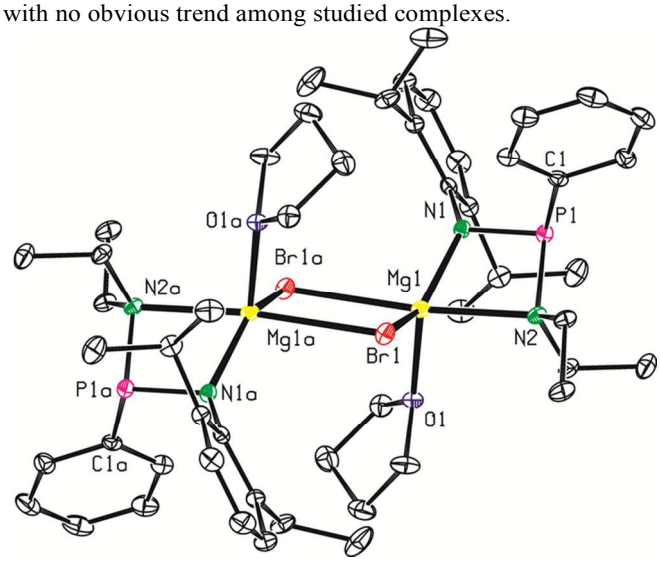

Figure 14 Molecular structure of **12** (40% probability displacement ellipsoids, only one of two independent molecules in the unit cell is shown). Hydrogen atoms are omitted for clarity. The symmetry operator a = -x, 1-y, 1-z. Selected bond lengths [Å] and bonding angles [deg]: Mg(1)-N(1) 2.010(2), Mg(1)-N(2) 2.296(2), Mg(1)-Br(1) 2.5773(8), Mg(1)-Br(1a) 2.7089(9), Mg(1)-O(1) 2.0409(19), P(1)-N(1) 1.671(2), P(1)-N(2) 1.811(2), N(1)-Mg(1)-N(2) 72.89(8), N(1)-Mg(1)-Br(1) 134.48(7), N(1)-Mg(1)-Br(1a) 101.41(6), N(1)-Mg(1)-O(1) 118.50(8), N(2)-Mg(1)-Br(1) 97.09(6), N(2)-Mg(1)-Br(1a) 173.96(6), N(2)-Mg(1)-O(1) 95.44(8), Br(1)-Mg(1)-Br(1a) 85.50(2), Br(1)-Mg(1)-O(1) 106.45(6), Br(1a)-Mg(1)-O(1) 89.02(6), Mg(1)-Br(1)-Mg(1a) 94.50(3), N(1)-P(1)-N(2) 94.98(10).

Conclusions

We have demonstrated high potential of phosphanes **1-3** as ligand-precursors for the preparation of magnesium compounds by a simple metallation using *n*-Bu_2Mg and MeMgBr. The structural versatility of isolated products is remarkable and importantly, an isolation of a particular structural motif may be controlled by a targeted substitution of the respective phosphane. Another approach is the utilization of the NH→PH tautomeric shift as a useful tool for the preparation of monoanionic NPN phosphinate backbone. Significant benefit of **1-3** and their derivatives is an easy and straightforward monitoring of experimental procedures by ^{31}P NMR spectroscopy. The extension of utilization of **1-3** and related systems in the main group chemistry is a next target for us.

Experimental

General procedures

All air and moisture sensitive manipulations were carried out under an argon atmosphere using standard Schlenk tube technique. All solvents were dried using Pure Solv–Innovative Technology equipment. The starting compounds: *n*-Bu_2Mg (1 M solution in heptane) and MeMgBr (1.4 M solution in THF/toluene 3:1) were obtained from the commercial suppliers and used as delivered. The ligand-precursors **1** and **2** were prepared according to published procedures.[11] ^{1}H, ^{13}C{^{1}H} and ^{31}P NMR spectra were recorded on a Bruker Avance 500 or a Bruker Avance III 400 MHz spectrometers, using a 5 mm tunable broad-band probe. Appropriate chemical shifts in ^{1}H and ^{13}C{^{1}H} NMR spectra were related to the residual signals of the solvent [C_6D_6: δ(^{1}H) = 7.16 ppm and δ(^{13}C) = 128.39 ppm, THF-d8: δ(^{1}H) = 3.58 ppm and δ(^{13}C) = 67.57 ppm], ^{31}P NMR chemical shifts were referred to external 85% H_3PO_4. ^{31}P-^{31}P EXSY of compound **10** without and with free ligand in THF-D_8 were measured using mixing time being from 0.1 to 1.5 s and applying standard NOESY pulse program provided by the NMR spectrometer producer (TOPSPIN 2.1). Appropriate cross-peaks had positive phases. Elemental analyses were performed on an LECO-CHNS-932 analyzer.

Syntheses

Synthesis of PhP(NEt$_2$)(NHDip) (3): Et_2NH (5.88 mL, 56.1 mmol) was dissolved in diethylether (100 mL) and a solution of PhP(NHDip)Cl (7.979 g, 24.9 mmol) in diethylether (50 mL) was added at 0°C while stirring. A precipitate formed. Stirring continued overnight, the solid was removed by filtration and washed three times with 50 mL of diethylether. The solutions were combined and the solvent and the excess amine were removed *in vacuo* giving colourless crystals of **3**. Yield 91%; m.p. 58-59°C. ^{1}H NMR (400MHz, C_6D_6, 25°C): δ = 0.81 (t, $^3J_{H-H}$ = 7.2 Hz, 6H, CH_2CH_3), 1.25 (d, $^3J_{H-H}$ = 6.8 Hz, 6H, $CHCH_3$), 1.27 (d, $^3J_{H-H}$ = 6.8 Hz, 6H, $CHCH_3$), 2.87 (m, 4H, CH_2CH_3), 3.53 (sept, $^3J_{H-H}$ = 6.8 Hz, 6H, $CHCH_3$), 4.28 (d, $^2J_{P-H}$ = 5.6 Hz, 1H, N*H*), 7.16 (m, 4H, Ar-*H*), 7.28 (t, 2H, Ar-*H*), 7.84 (m, 2H, Ar-*H*) ppm. ^{13}C{^{1}H} NMR (100.61MHz, C_6D_6, 25°C): δ = 15.6 (s, CH_2CH_3), 24.4 (s, $CHCH_3$), 24.8 (s, $CHCH_3$), 28.8 (s, $CHCH_3$), 43.2 (d, $^2J_{P-C}$ = 16.1 Hz, CH_2CH_3), 124.3 (s, Ar-*C*), 124.4 (s, Ar-*C*), 128.8 (s, Ar-*C*), 129.0 (d, J_{P-C} = 3.8 Hz, Ar-*C*), 131.4 (d, J_{P-C} = 16.2 Hz, *o*-C_6H_5), 140.3 (d, $^1J_{P-C}$ = 10.8 Hz, *ipso*-*C*), 142.8 (d, J_{P-C} = 4.6 Hz, Ar-*C*), 143.4 (s, Ar-*C*) ppm. ^{31}P NMR (161.97MHz, C_6D_6, 25°C): δ = 82.5 (s) ppm. Anal. calcd. for $C_{22}H_{33}N_2P$ (356.50): C 74.1, H 9.3; found C 74.2, H 9.4.

Synthesis of [PhP(NH*t*-Bu)(N*t*-Bu)]Mg(*n*-Bu) (4): *n*-Bu_2Mg (3.4 mL, 3.4 mmol, 1 M solution in heptane) was added dropwise to a solution of **1** (0.869 g, 3.4 mmol) in hexane (20 mL) at -40°C while stirring. The reaction mixture was slowly warmed to room temperature and stirred for one hour. The yellowish solution was concentrated to approximately one third and stored at 6°C for one day, yielding colourless crystals of **4**. Yield 401 mg, 35%; m.p. 107°C. ^{1}H NMR (400MHz, C_6D_6, 25°C): δ = 0.16 (t, 2H, *n*-Bu-CH_2Mg), 0.88 (s, 9H, $C(CH_3)_3$), 1.24 – 1.60, 1.85 – 2.11 (m, 8H, *n*-Bu, N*H*), 1.71 (s, 9H, $C(CH_3)_3$), 6.96 (t, 1H, Ar-*H*), 7.13 (m, 2H, Ar-*H*), 7.53 (m, 2H, Ar-*H*) ppm. ^{13}C{^{1}H} NMR (100.61MHz, C_6D_6, 25°C): δ = 14.8 (s, $MgCH_2CH_2CH_2CH_3$), 16.1 (s, $MgCH_2CH_2CH_2CH_3$), 31.2 (d, $^3J_{P-C}$ = 9.8 Hz, $C(CH_3)_3$), 33.0 and 33.6 (s, $CH_2CH_2CH_2CH_3$), 35.3 (d, $^3J_{P-C}$ = 13.7 Hz, $C(CH_3)_3$), 54.5 (d, $^2J_{P-C}$ = 22.0 Hz, $C(CH_3)_3$), 56.9 (d, $^2J_{P-C}$ = 31.7 Hz, $C(CH_3)_3$), 129.1 (s, Ar-*C*), 129.8 (d, $^2J_{P-C}$ = 18.2 Hz, *o*-C_6H_5), 130.5 (s, Ar-*C*), 148.3 (d, $^1J_{P-C}$ = 33.8 Hz, *ipso*-*C*) ppm. ^{31}P NMR

(161.97MHz, C_6D_6, 25°C): δ = 88.3 (s) ppm. Anal. calcd. for $C_{18}H_{33}MgN_2P$ (332.76): C 65.0, H 10.0; found C 65.1, H 10.1.

Synthesis of [PhP(NH*t*-Bu)(N*t*-Bu)]$_2$Mg (5): *n*-Bu_2Mg (1.5 mL, 1.5 mmol, 1 M solution in heptane) was added dropwise to a solution of **1** (0.762 g, 3.0 mmol) in hexane (20 mL) at -40°C while stirring. The reaction mixture was slowly warmed to room temperature and stirred for one hour. The slightly yellow solution was concentrated to approximately one third and stored at 6°C for one day, yielding colourless single-crystals of **5**. Yield 414 mg, 52%; m.p. 166°C. ^{1}H NMR (400MHz, C_6D_6, 25°C): δ = 1.05 (s broad, 18H, C(CH_3)$_3$), 1.57 (s, 18H, C(CH_3)$_3$), 1.86 (s, 2H, N*H*), 7.10 – 7.29 (m broad, 6H, Ar-*H*), 7.88 (m broad, 4H, Ar-*H*) ppm. ^{13}C{^{1}H} NMR (100.61MHz, C_6D_6, 25°C): δ = 31.2 (s broad, C(*C*H$_3$)$_3$), 36.3 (d, $^3J_{P\text{-}C}$ = 11.3 Hz, C(*C*H$_3$)$_3$), 52.7 (d, $^2J_{P\text{-}C}$ = 18.7 Hz, *C*(CH$_3$)$_3$), 56.9 (s broad, *C*(CH$_3$)$_3$), 128.8 (s, *p*-C_6H_5), 130.1 (d, $^2J_{P\text{-}C}$ = 20.0 Hz, *o*-C_6H_5), 131.1 (d, $^3J_{P\text{-}C}$ = 17.2 Hz, *m*-C_6H_5), *ipso-C* not observed ppm. ^{31}P NMR (161.97MHz, C_6D_6, 25°C): δ = 92.5 (s) ppm. Anal. calcd. for $C_{28}H_{48}MgN_4P_2$ (526.98): C 63.8, H 9.2; found C 63.7, H 9.1.

Synthesis of [PhP(NH*t*-Bu)N(*t*-Bu)]MgBr.(THF) (6): MeMgBr (1.5 mL, 2.1 mmol, 1.4 M solution in THF/toluene 3:1) was added dropwise to a solution of **1** (0.522 g, 2.1 mmol) in THF (20 mL) at -40°C while stirring. Small bubbles of methane appeared and the solution turned yellow. The reaction mixture was slowly warmed to room temperature and stirred for one hour and the solution turned to colourless again. The solvent was removed under *vacuo* to yield colourless oil of **6**. Yield 414 mg, 95%. ^{1}H NMR (400MHz, C_6D_6, 25°C): δ = 1.14 (m, 4H, C_4H_8O), 1.34 (s, 9H, C(CH_3)$_3$), 1.57 (s, 9H, C(CH_3)$_3$), 1.80 (s, 1H, N*H*), 3.55 (m, 4H, C_4H_8O), 7.12 (m, 1H, Ar-*H*), 7.23 (m, 2H, Ar-*H*), 7.81 (t, 2H, Ar-*H*) ppm. ^{13}C{^{1}H} NMR (100.61MHz, C_6D_6, 25°C): δ = 25.3 (s, C_4H_8O), 31.2 (d, $^3J_{P\text{-}C}$ = 9.0 Hz, C(*C*H$_3$)$_3$), 35.9 (d, $^3J_{P\text{-}C}$ = 10.5 Hz, C(*C*H$_3$)$_3$), 52.4 (d broad, $^2J_{P\text{-}C}$ = 26.6 Hz, *C*(CH$_3$)$_3$), 53.6 (d broad, $^2J_{P\text{-}C}$ = 15.8 Hz, *C*(CH$_3$)$_3$), 69.7 (s, C_4H_8O), 128.6 (d, $^3J_{P\text{-}C}$ = 4.3 Hz, *m*-C_6H_5), 128.7 (s, *p*-C_6H_5), 129.7 (d, $^2J_{P\text{-}C}$ = 19.6 Hz, *o*-C_6H_5), 152.9 (d, $^1J_{P\text{-}C}$ = 43.5 Hz, *ipso*-C_6H_5) ppm. ^{31}P NMR (161.97MHz, C_6D_6, 25°C): δ = 89.1 (s) ppm.

Synthesis of [Ph(H)P(N*t*-Bu)$_2$]$_2$Mg (7): MeMgBr (1.9 mL, 2.7 mmol, 1.4 M solution in THF/toluene 3:1) was added dropwise to a solution of **1** (0.687 g, 2.7 mmol) in THF (20 mL) at -40°C while stirring. Small bubbles of methane appeared and the solution turned yellow. The reaction mixture was slowly warmed to room temperature and stirred for one hour and the solution turned to colourless again. The solvent was removed under reduced pressure and the product was re-dissolved in toluene (5 mL) and stored at -30°C for one day yielding colourless single-crystals of **7**. Yield 459 mg, 64%; m.p. 155°C. ^{1}H NMR (400MHz, C_6D_6, 25°C): δ = 1.28 (s, 18H, C(CH_3)$_3$), 1.35 (s, 18H, C(CH_3)$_3$), 7.04 – 7.15 (m, 6H, Ar-*H*), 7.62 (m, 4H, Ar-*H*), 7.76 (d, $^1J_{P\text{-}H}$ = 431.7 Hz, 2H, P*H*) ppm. ^{13}C{^{1}H} NMR (100.61MHz, C_6D_6, 25°C): δ = 35.3 (d, $^3J_{P\text{-}C}$ = 9.7 Hz, C(*C*H$_3$)$_3$), 35.5 (d, $^3J_{P\text{-}C}$ = 9.8 Hz, C(*C*H$_3$)$_3$), 50.7 (d, $^2J_{P\text{-}C}$ = 5.8 Hz, *C*(CH$_3$)$_3$) the signal of the carbon atom of the second *C*(CH$_3$)$_3$ was not observed probably due to the significant broadening, 129.0 (d, $J_{P\text{-}C}$ = 11.8 Hz, Ar-*C*), 130.1 (d, $J_{P\text{-}C}$ = 20.0 Hz, Ar-*C*), 131.3 (s, Ar-*C*), 142.4 (d, $^1J_{P\text{-}C}$ = 82.4 Hz, *ipso*-C_6H_5) ppm. ^{31}P NMR (161.97MHz, C_6D_6, 25°C): δ = 8.9 (d, $^1J_{P\text{-}H}$ = 431.7 Hz) ppm. Anal. calcd. for $C_{28}H_{48}MgN_4P_2$ (526.98): C 63.8, H 9.2; found C 63.9, H 9.2.

{[PhP(NPh)$_2$]$_2$Mg(THF)$_2$}$_2$ (8): *n*-Bu_2Mg (1.5 mL, 1.5 mmol, 1 M solution in heptane) was added dropwise to a solution of **2** (0.452 g, 1.5 mmol) in THF/toluene (1:1, 20 mL) at -70°C while stirring. The reaction mixture was slowly warmed to room temperature and stirred for one hour. Slightly yellow precipitate is formed during warming. The suspension was filtrated and washed three times with 30 mL of THF at 50°C (to remove traces of a side product **9** see discussion) giving slightly yellow powder of **8**. Single-crystals of **8** were grown in benezene. Yield 419 mg, 59%; m.p. 175°C with decomposition. ^{1}H NMR (400MHz, C_6D_6, 25°C): δ = 1.10 (s broad, 8H, C_4H_8O), 3.31 (s, broad, 8H, C_4H_8O), 6.71 (t, 2H, Ar-*H*), 7.01 (m, 2H, Ar-*H*), 7.14 – 7.19 (m, 5H, Ar-*H*), 7.47 (d, 4H, Ar-*H*) 8.03 (m, 2H, Ar-*H*) ppm. ^{13}C{^{1}H} NMR (100.61MHz, C_6D_6, 25°C): δ = 25.5 (s, C_4H_8O), 69.8 (s, C_4H_8O), 116.6 (s, Ar-*C*), 121.6 (d, $J_{P\text{-}C}$ = 19.9 Hz, Ar-*C*), 128.8 (d, $J_{P\text{-}C}$ = 3.9 Hz, Ar-*C*), 129.5 (s, Ar-*C*), 129.7 (s, Ar-*C*), 131.0 (d, $J_{P\text{-}C}$ = 19.2 Hz, Ar-*C*), 150.1 (d, $^1J_{P\text{-}C}$ = 53.4 Hz, *ipso*-C_6H_5P), 155.9 (d, $^2J_{P\text{-}C}$ = 13.1 Hz, *ipso*-C_6H_5N) ppm. ^{31}P NMR (161.97MHz, C_6D_6, 25°C): δ = 93.3 (s) ppm. Anal. calcd. for $C_{26}H_{31}MgN_2O_2P$ (458.84): C 68.1, H 6.8; found C 68.2, H 6.9.

[Ph(H)P(NPh)$_2$]$_2$Mg(THF) (9): *n*-Bu_2Mg (1.2 mL, 1.2 mmol, 1 M solution in heptane) was added dropwise to a solution of **2**(0.694 g, 2.4 mmol) in THF (20 mL) at -10°C while stirring. The reaction mixture was slowly warmed to room temperature and stirred for one hour. The solvent was removed under reduced pressure and the product was re-dissolved in toluene and stored at -30°C to give single-crystals of **9**. Yield 339 mg, 42%; m.p. 96°C. ^{1}H NMR (400MHz, C_6D_6, 25°C): δ = 1.27 (s broad, 8H, C_4H_8O), 3.63 (s, broad, 8H, C_4H_8O), 6.70 (t, 4H, Ar-*H*), 6.93 – 7.11 (m, 22H, Ar-*H*), 7.82 (dd, 2H, Ar-*H*) 7.84 (dd, 2H, Ar-*H*), 8.31 (d, $^1J_{P\text{-}H}$ = 442.2 Hz, 2H, P*H*) ppm. ^{13}C{^{1}H} NMR (100.61MHz, C_6D_6, 25°C): δ = 25.8 (s, C_4H_8O), 68.9 (s, C_4H_8O), 118.9 (s, Ar-*C*), 121.6 (d, $J_{P\text{-}C}$ = 18.4 Hz, Ar-*C*), 129.6 (d, $J_{P\text{-}C}$ = 12.7 Hz, Ar-*C*), 129.7 (s, Ar-*C*), 130.8 (d, $J_{P\text{-}C}$ = 12.1 Hz, Ar-*C*), 132.6 (s, Ar-*C*), 133.3 (d, $^1J_{P\text{-}C}$ = 91.8 Hz, *ipso*-C_6H_5P), 149.7 (s, *ipso*-C_6H_5N) ppm. ^{31}P NMR (161.97MHz, C_6D_6, 25°C): δ = 11.6 (d, $^1J_{P\text{-}H}$ = 442.2 Hz) ppm. Anal. calcd. for $C_{40}H_{40}MgN_4OP_2$ (679.05): C 70.8, H 5.9; found C 70.8, H 5.9.

[Ph(H)P(NPh)$_2$]MgBr(THF)$_2$ (10): MeMgBr (2.0 mL, 2.8 mmol, 1.4 M solution in THF/toluene 3:1) was added dropwise to a solution of **2** (0.804 g, 2.8 mmol) in THF (20 mL) at -70°C while stirring. The reaction mixture was slowly warmed to room temperature and stirred for one hour. The solvent was removed under reduced pressure and the product was recrystallized from toluene giving single crystals of **10**. Yield 1.128 g, 76%; m.p. 100-101°C. ^{1}H NMR (400MHz, THF-d_8, 25°C): ^{1}H NMR spectrum contained two sets of signals, major set: δ = 7.87 (dd, 2H, Ar-*H*), 8.27 (d, 1H, $^1J_{P\text{-}H}$ = 444.3 Hz, P*H*), minor set: δ = 7.70 (dd, 2H, Ar-*H*), 8.16 (d, 1H, $^1J_{P\text{-}H}$ = 439.9

Hz, P*H*) ppm. The ^{1}H NMR spectrum also contained: δ = 1.71 (s broad, 8H, C_4H_8O), 3.58 (s, broad, 8H, C_4H_8O), 6.11 (s broad, Ar-*H*), 6.47 (d, Ar-*H*), 6.64 (t, Ar-*H*) 6.77 – 7.03 (m, Ar-*H*), 7.25 – 7.39 (m, Ar-*H*), 7.59 (t, Ar-*H*) ppm. ^{13}C{^{1}H} NMR (100.61MHz, THF-d_8, 25°C): δ = 26.4 (s, C_4H_8O), 68.4 (s, C_4H_8O), 117.3 (d, J_{P-C} = 12.4 Hz, Ar-*C*), 118.4 (d, J_{P-C} = 41.1 Hz, Ar-*C*), 119.8 (s, Ar-*C*), 121.7 (d, J_{P-C} = 18.5 Hz, Ar-*C*), 122.8 (d, J_{P-C} = 16.8 Hz, Ar-*C*), 129.3 (d, J_{P-C} = 17.9 Hz, Ar-*C*), 129.7 (s, Ar-*C*), 130.9 (d, J_{P-C} = 17.9 Hz, Ar-*C*), 131.4 (d, J_{P-C} = 11.7 Hz, Ar-*C*), 132.6 (d, J_{P-C} = 2.6 Hz, Ar-*C*), 132.8 (d, J_{P-C} = 2.5 Hz, Ar-*C*), 134.1 (d, J_{P-C} = 91.0 Hz, *ipso*-C_6H_5P), 150.4 (d, J_{P-C} = 53.5 Hz, *ipso*-C_6H_5N) ppm. ^{31}P NMR (161.97MHz, THF-d_8, 25°C): ^{31}P NMR spectrum contained two signals, major signal: δ = 9.3 (d, $^{1}J_{P-H}$ = 444.3 Hz), minor signal: δ = 8.9 (d, $^{1}J_{P-H}$ = 439.9 Hz) ppm. Anal. calcd. for $C_{26}H_{32}BrMgN_2O_2P$ (539.75): C 57.9, H 6.0; found C 58.0, H 6.1.

[PhP(NEt$_2$)(NDip)]$_2$Mg (**11**): *n*-Bu_2Mg (1.4 mL, 1.4 mmol, 1 M solution in heptane) was added dropwise to a solution of **3** (0.502 g, 1.4 mmol) in hexane (30 mL) at -40°C while stirring. The reaction mixture was slowly warmed to room temperature and stirred for one hour. The colourless solution was concentrated to approximately half of its volume and stored at 6°C for one day, yielding colorless single-crystals of **11**. Yield 254 mg, 49%; m.p. 140°C. ^{1}H NMR (400MHz, C_6D_6, 25°C): δ = 0.73 (m broad, 6H, CHCH_3), 0.85 (m broad, 6H, CHCH_3), 1.20 (m broad, 6H, CHCH_3), 1.39 (m broad, 6H, CHCH_3), 2.11 (m broad, 12H, CH_2CH_3), 3.20 (m broad, 4H, CH_2CH$_3$), 3.54 (m broad, 2H, C*H*CH$_3$), 3.74 (m broad, 2H, C*H*CH$_3$), 3.93 (m broad, 4H, CH_2CH$_3$), 6.93 (t, 4H, Ar-*H*), 7.02 (t, 2H, Ar-*H*), 7.10 (m, 2H, Ar-*H*), 7.12 (m, 4H, Ar-*H*), 7.77 (m, 4H, Ar-*H*) ppm. ^{13}C{^{1}H} NMR (100.61MHz, C_6D_6, 25°C): δ = 23.0 (s, broad, *C*HCH_3), 24.8 (s broad, *C*HCH_3), 26.7 (s broad, *C*HCH_3), 27.3 (s broad, *C*HCH$_3$), 28.2 (s broad, *C*HCH_3), 29.6 (s broad, *C*HCH$_3$), 42.6 (s, *C*H_2CH$_3$), 42.7 (s, *C*H_2CH$_3$), 122.7 (s, Ar-*C*), 123.9 (s, Ar-*C*), 124.3 (s, Ar-*C*), 128.8 (d, J_{P-C} = 6.7 Hz, Ar-*C*), 130.3 (s, Ar-*C*), 131.8 (d, J_{P-C} = 26.5 Hz, Ar-*C*), 145.7 (d, J_{P-C} = 48.4 Hz, Ar-*C*), 147.2 (d, J_{P-C} = 20.1 Hz, Ar-*C*), 147.3 (s, Ar-*C*) ppm. ^{31}P NMR (161.97MHz, C_6D_6, 25°C): δ = 122.1 (s) ppm. Anal. calcd. for $C_{44}H_{64}MgN_4P_2$ (735.29): C 71.9, H 8.8; found C 71.9, H 8.8.

{[PhP(NEt$_2$)(NDip)$_2$]Mg(μ-Br)(THF)}$_2$ (**12**): MeMgBr (1.3 mL, 1.8 mmol, 1.4 M solution in THF/toluene 3:1) was added dropwise to a solution of **3** (0.633 g, 1.8 mmol) in THF (20 mL) at -70°C while stirring. The reaction mixture was slowly warmed to room temperature and stirred for three hours. The solvent was removed under reduced pressure and the product was recrystallized from toluene giving single crystals of **12**. Yield 0,465 g, 69%; m.p. 121°C. ^{1}H NMR (400MHz, C_6D_6, 25°C): δ = 0.96 (t, $^{3}J_{H-H}$ = 7.0 Hz, 6H, CH_2CH_3), 1.07 (s broad, 4H, C_4H_8O), 1.22 (d, $^{3}J_{H-H}$= 6.8 Hz, 6H, CHCH_3), 1.43 (d, $^{3}J_{H-H}$= 6.8 Hz, 6H, CHCH_3), 2.88 (m broad, 2H, CH_2CH$_3$), 3.12 (m broad, 2H, CH_2CH$_3$), 3.57 (s broad, 4H, C_4H_8O) 4.23 (sept, $^{3}J_{H-H}$= 6.8 Hz, 6H, C*H*CH$_3$), 7.01 (m, 1H, Ar-*H*), 7.11 – 7.16 (m, 3H, Ar-*H*), 7.24 (t, 2H, Ar-*H*), 8.08 (t, 2H, Ar-*H*) ppm. ^{13}C{^{1}H} NMR (100.61MHz, C_6D_6, 25°C): δ = 12.6 (d, $^{3}J_{P-C}$ = 6.6 Hz, CH_2CH_3), 25.2 (s, C_4H_8O), 25.5 (s, *C*HCH_3), 26.1 (s, *C*HCH_3), 28.8 (s, *C*HCH_3), 43.3 (d, $^{2}J_{P-C}$ = 14.1 Hz, *C*H_2CH$_3$), 70.5 (s, C_4H_8O), 122.0 (s, Ar-*C*), 124.3 (s, Ar-*C*), 128.5 (d, J_{P-C} = 7.1 Hz, Ar-*C*), 129.9 (s, Ar-*C*), 133.0 (d, J_{P-C} = 27.7 Hz, *o*-C_6H_5), 145.3 (d, $^{1}J_{P-C}$ = 49.2 Hz, *ipso*-C_6H_5), 145.4 (s, Ar-*C*), 147.3 (s, Ar-*C*) ppm. ^{31}P NMR (161.97MHz, C_6D_6, 25°C): δ = 127.6 (s broad) ppm. Anal. calcd. for $C_{26}H_{40}BrMgN_2OP$ (531.81): C 58.7, H 7.6; found C 58.8, H 7.6.

Computational Details

All the calculations were performed with the Gaussian 09 program[20] using the dispersion-corrected B3LYP-D functional[21] together with the Dunning´s correlation consistent basis sets.[22] The Grimme D dispersion correction[23] was applied throughout. The geometries of all species were fully optimized and characterized by harmonic vibrational frequency computations at the B3LYP-D/aug-cc-pVDZ level. Thermal contributions to the enthalpy and Gibbs free energy at 298 K were obtained by standard thermodynamics calculations at the B3LYP-D/aug-cc-pVDZ level. More reliable relative energies were obtained from single-point calculations at the B3LYP-D/aug-cc-pVTZ level. The performance of the B3LYP-D hybrid functional on the geometries and relative energies of isomers of **10** was assessed by comparison with experiment. We also performed all calculations with the M06 functional[24] and BP86-D functional.[25]

Implicit solvent effects were computed using the polarizable continuum model (PCM) with radii and non-electrostatic terms from Truhlar and co-workers' SMD model[26] at the B3LYP-D/aug-cc-pVTZ level of theory. The ^{31}P magnetic shielding tensors of the optimized structures in THF were computed with the Gauge-Independent Atomic Orbital (GIAO) method at the B3LYP/cc-pVTZ level of theory. To compare isotropic shieldings with the experimentally observed ^{31}P chemical shifts, the NMR parameters for H_3PO_4 were calculated at the same level of theory and used as the reference molecule.

X-ray crystallography

The suitable single crystals of **5** and **7-12** were mounted on a glass fibre with an oil and measured on a four-circle diffractometer KappaCCD with a CCD area detector by monochromatized MoK_α radiation (λ = 0.71073 Å) at 150(1) K. The numerical[28] absorption corrections from the crystal shape were applied for all crystals. The structures were solved by the direct method (SIR92)[29] and refined by a full matrix least squares procedure based on F^2 (SHELXL97).[30] Hydrogen atoms were fixed into idealized positions (riding model) and assigned temperature factors H_{iso} (H) = 1.2 Ueq (pivot atom) or of 1.5 U_{eq} for the methyl moiety with C–H = 0.96, 0.97, 0.98 and 0.93 Å for methyl, methylene, methine and hydrogen atoms in the aromatic ring, respectively. The hydrogen atoms of NH and PH groups were refined from the Fourier difference map. Two carbon atoms of disorder THF molecule coordinated to the magnesium atom in **8a** was split into two positions. There are disordered solvent molecules (THF) of **8a** and **9**. Attempts were made to model this disorder, but were unsuccessful. PLATON

/SQUEZZE[31] software was used to correct the data for the presence of disordered solvent. In the case of **8a**, a potential solvent volume of 304 Å^3 was found. 100 electrons per unit cell worth of scattering were located in the void. The calculated stoichiometry of solvent was calculated to be two molecule of THF per unit cell, which results in 80 electrons per unit cell. In the case of **9**, a potential solvent volume of 312 Å^3 was found. 87 electrons per unit cell worth of scattering were located in the void. The calculated stoichiometry of solvent was calculated to be two molecule of THF per unit cell which results in 80 electrons per unit cell. Crystallographic data for structural analysis has been deposited with the Cambridge Crystallographic Data Centre, CCDC nos. 1039909-1039916.

Crystallographic data for 5. $C_{28}H_{48}MgN_4P_2$, M = 526.95, monoclinic, $P2_1/c$, a = 17.4962(4), b = 11.4130(2), c = 18.2113(6) Å, β = 121.211(2)°, V = 3110.18(15) Å^3, Z = 4, T = 150(1) K, 24498 total reflections, 6869 independent (R_{int} = 0.029, $R1$ (obs. data) = 0.038, w$R2$ (all data) 0.084), S = 1.156, Δρ, max., min. [e Å^{-3}] 0.332, -0.307, CCDC 1039914.

Crystallographic data for 7. $C_{28}H_{48}MgN_4P_2$, M = 526.95, $C2/c$, a = 25.7012(3), b = 8.6979(5), c = 18.7740(2) Å, β = 132.402(3)°, V = 3099.1(15) Å^3, Z = 4, T = 150(1) K, 10544 total reflections, 2959 independent (R_{int} = 0.028, $R1$ (obs. data) = 0.038, w$R2$ (all data) 0.100), S = 1.174, Δρ, max., min. [e Å^{-3}] 0.339, -0.421, CCDC 1039911.

Crystallographic data for 8. $C_{52}H_{62}Mg_2N_4O_4P_2.(2C_6H_6)$, M = 1073.83, triclinic, $P\text{-}1$, a = 10.9041(7), b = 11.0920(5), c = 12.5151(8) Å, α = 97.568(5), β = 91.018(5), γ = 110.470(4)°, V = 1402.33(14) Å^3, Z = 1, T = 150(1) K, 27272 total reflections, 5404 independent (R_{int} = 0.024, $R1$ (obs. data) = 0.040, w$R2$ (all data) 0.099), S = 1.087, Δρ, max., min. [e Å^{-3}] 0.493, -0.413, CCDC 1039909.

Crystallographic data for 8a. $C_{30}H_{39}MgN_2O_3P.C_4H_8O$, M = 603.01, monoclinic, Pc, a = 11.8910(9), b = 17.7050(12), c = 15.8581(13) Å, β = 102.911(6)°, V = 3254.2(4) Å^3, Z = 4, T = 150(1) K, 28458 total reflections, 10329 independent (R_{int} = 0.064, $R1$ (obs. data) = 0.070, w$R2$ (all data) 0.149), S = 1.131, Δρ, max., min. [e Å^{-3}] 0.512, -0.602, CCDC 1039913.

Crystallographic data for 9. $C_{40}H_{40}MgN_4OP_2.C_7H_8.C_4H_8O$, M = 846.24, triclinic, $P\text{-}1$, a = 10.0290(7), b = 12.7811(10), c = 19.548(2) Å, α = 84.135(8), β = 82.017(7), γ = 69.490(5)°, V = 2320.3(4) Å^3, Z = 2, T = 150(1) K, 45837 total reflections, 7802 independent (R_{int} = 0.038, $R1$ (obs. data) = 0.056, w$R2$ (all data) 0.141), S = 1.009, Δρ, max., min. [e Å^{-3}] 0.795, -0.419, CCDC 1039916.

Crystallographic data for 10. $C_{26}H_{32}BrMgN_2O_2P$, M = 305.25, monoclinic, $P2_1/c$, a = 11.0410(7), b = 23.3141(16), c = 11.5729(14) Å, β = 119.760(5)°, V = 2586.1(4) Å^3, Z = 4, T = 150(1) K, 16999 total reflections, 4543 independent (R_{int} = 0.040, $R1$ (obs. data) = 0.039, w$R2$ (all data) 0.094), S = 1.177, Δρ, max., min. [e Å^{-3}] 0.414, -0.550, CCDC 1039912.

Crystallographic data for 11. $C_{44}H_{64}MgN_4P_2$, M = 735.24, triclinic, $P\text{-}1$, a = 10.4730(8), b = 10.8549(8), c = 19.6561(15) Å, α = 91.260(7), β = 103.789(6), γ = 100.707(7)°, V = 2127.2(3) Å^3, Z = 2, T = 150(1) K, 34767 total reflections, 8002 independent (R_{int} = 0.026, $R1$ (obs. data) = 0.039, w$R2$ (all data) 0.088), S = 1.116, Δρ, max., min. [e Å^{-3}] 0.360, -0.296, CCDC 1039910.

Crystallographic data for 12. $C_{52}H_{80}Br_2Mg_2N_4O_2P_2$, M = 1063.58, triclinic, $P\text{-}1$, a = 12.1820(9), b = 14.8989(10), c = 16.3201(11) Å, α = 75.236(5), β = 71.290(4), γ = 82.394(6)°, V = 2708.8(3) Å^3, Z = 2, T = 150(1) K, 55308 total reflections, 9711 independent (R_{int} = 0.041, $R1$ (obs. data) = 0.037, w$R2$ (all data) 0.074), S = 1.134, Δρ, max., min. [e Å^{-3}] 0.421, -0.458, CCDC 1039915.

Acknowledgements

The authors thank the Grant agency of the Czech Republic project no. P207/12/0223. M. A. thanks the European Community for financial support through the postdoctoral fellowship FP7-PEOPLE-2010-IEF-273527. F. D. P wishes to thank the Fund for Scientific Research–Flanders (FWO) and the Free University of Brussels (VUB) for their continuous support.

Notes and references

[a] Department of General and Inorganic Chemistry, Faculty of Chemical Technology, University of Pardubice, Studentská 573, CZ - 532 10, Pardubice, Czech Republic Fax: +420466037068; Tel: +420466037163; E-mail: libor.dostal@upce.cz

[b] Eenheid Algemene Chemie (ALGC), Vrije Universiteit Brussel (VUB) Pleinlaan 2, B-1050 Brussels, Belgium

[c] Research Institute for Organic Syntheses, Rybitví 296, CZ-533 54 Pardubice, Czech Republic

† Electronic Supplementary Information (ESI) available: See DOI: 10.1039/b000000x/

1 For reviews see: (a) F.T. Edelmann, *Adv. Organomet. Chem.*, 2008, **57**, 183; (b) M. Asay, C. Jones and M. Driess, *Chem. Rev*., 2011, **221**, 354; (c) S. Collins, *Coord. Chem. Rev.*, 2011, **255**, 118; (d) A.A. Mohamed, *Coord. Chem. Rev.*, 2010, **254**, 1918; (e) F.T. Edelmann, *Chem. Soc. Rev.*, 2009, **38**, 2253; (f) J. Barker and M. Kilner, *Coord. Chem. Rev*., 1994, **133**, 219.

2 (a) P.J. Bailey and S. Pace, *Coord. Chem. Rev.*, 2001, **214**, 91; (b) M.P. Coles, *Chem. Commun*., 2009, 3659.

3 C. Fedorchuk, M. Copsey and T. Chivers, *Coord. Chem. Rev.*, 2007, **251**, 897.

4 For some recent examples see: (a) R.J. Schwamm, B.M. Day, M.P. Coles and C.M. Fitchett, *Inorg. Chem.*, 2014, **53**, 3778; (b) D.R. Amstrong, W. Clegg, A. Hernan-Gomez, A.R. Kennedy, Z. Livingstone, S.D. Robertson, L. Russo and E. Hevia, *Dalton Trans.*, 2014, **43**, 4361; (c) B.J. Day and M.P. Coles, *Organometallics*, 2013, **32**, 4270; (d) B.J. Day, P.W. Dyer and M.P. Coles, *Dalton Trans.*, 2012, **41**, 7457; (e) J.K. West and L. Stahl, *Organometallics*, 2012, **31**, 2042; (g) A. Mane, C. Wagner and K. Merzweiler, *Z. Anorg. Allg. Chem.*, 2012, **638**, 136; (h) D. Yang, J. Guo, H. Wu, Y. Ding and W. Zheng, *Dalton Trans.*, 2012, **41**, 2187; (i) D.-Y. Lu, J.-S. Yu, T.-S. Kuo, G.-H. Lee, Y. Wang and Y.-C. Tsai, *Angew. Chem., Int. Ed.*, 2011, **50**, 7611; (j) C.-L. Pan, W. Chen and J. Song, *Organometallics*, 2011, **30**, 2252.

5 For example see: (a) G.G. Briand, T. Chivers, M. Krahn and M. Parvez, *Inorg. Chem.*, 2002, **41**, 6808; (b) S. Peitz, N. Peulecke, B.R. Aluri, S. Hansen, B.H. Müller, A. Spannenberg, U. Rosenthal, M.H. Al-Hazmi, F.M. Mosa, A. Wöhl and W. Müller, *Eur. J. Inorg. Chem.*,

2010, 1167; (c) C. Qi and Z. Wang, *J. Polymer Sci: Part A: Polymer Chem.*, 2006, **44**, 4621; (d) S.A. Ahmed, M.S. Hill, P.B. Hitchcock, S.M. Mansell and O. St John, *Organometallics*, 2007, **26**, 538; (e) B.H. Müller, N. Peulecke, A. Spannenberg, U. Rosenthal, M.H. Al-Hazmi, R. Schmidt, A. Wöhl and W. Müller, *Organometallics*, 2012, **31**, 3695; (f) K. Albahily, D. Al-Baldawi, S. Gambarotta, E. Koç and R. Duchateau, *Organometallics*, 2008, **27**, 5943. (g) K. Albahily, E. Koç, D. Al-Baldawi, D. Savard, S. Gambarotta, T.J. Burchell and R. Duchateau, *Angew. Chem., Int. Ed.*, 2008, **47**, 5816; (h) A. Stasch, *Chem. Eur. J.*, 2012, **18,** 15105; (i) B. Nekoueishahraki, H.W. Roesky, G. Schwab, D. Stern and D. Stalke, *Inorg. Chem.*, 2009, **48**, 9174. (j) B. Prashanth and S. Singh, *Dalton Trans.*, DOI: 10.1039/C4DT02637C

6 (a) T. Bauer, S. Schulz, M. Nieger and I. Krossing, *Chem. Eur. J.*, 2004, **10**, 1729; (b) T. Bauer, S. Chatterjee, S. Schulz, M. Nieger and I. Krossing, *Z. Allg. Anorg. Chem.*, 2005, **631**, 2900; (c) T. Bauer, S. Schulz, M. Nieger and I. Krossing, *Chem. Commun.*, 2002, 1422; (d) S. Schulz, M. Raab, M. Nieger and E. Niecke, *Organometallics*, 2000, **19**, 2616; (e) J.S. Ritch, T. Chivers, D.J. Eisler and H.M Tuononen, *Chem. Eur. J.*, 2007, **13**, 4643; (f) M. Raab, A. Sundermann, G. Schick, A. Loew, M. Nieger, W.W. Snoeller and E. Niecke, *Organometallics*, 2001, **20**, 1770.

7 J. Vrána, R. Jambor, A. Růžička, M. Alonso, F. De Proft and L. Dostál, *Eur. J. Inorg. Chem.*, 2014, 5193.

8 For example see: (a) R. Boomishankar, P.I. Richards, A.K. Gupta and A. Steiner, *Organometallics*, 2010, **29**, 2515; (b) I. Schranz, L. Stahl and R.J. Staples, *Inorg. Chem.* 1998, **37**,1493; (c) S.A. Ahmed, M.S. Hill and P.B. Hitchcock, *Organometallics*, 2006, **25**, 394; (d) E. Hollink, P. Wei and D.W. Stephan, *Can. J. Chem.*, 2005, **83**, 430; (e) A. Amstrong, T. Chivers, H.M. Tuononen and M. Parvez, *Inorg. Chem.*, 2005, **44**, 5778; (f) G.G. Briand, T. Chivers, M. Parvez and G. Schatte, *Inorg. Chem.*, 2003, **42**, 525; (h) D.A. Dickie, K.B. Gislason and R.A. Kemp, *Inorg. Chem.*, 2011, **51**, 1162.

9 (a) R. Fleischer and D. Stalke, *Inorg. Chem.*, 1997, **36**, 2413; (b) S.D. Robertson, T. Chivers and J. Konu, *J. Organomet. Chem.*, 2007, **692**, 4327.

10 A. Stasch, *Angew. Chem., Int. Ed.*, 2014, **53**, 10200.

11 B. Eichhorn, H. Nöth and T. Seifert, *Eur. J. Inorg. Chem.*, 1999, 2355.

12 T. Chivers, M. C. Copsey, C. Fedorchuk, M. Parvez and M. Stubbs, *Organometallics*, 2005, **24,** 1919.

13 (a) P. Pyykkö and M. Atsumi, *Chem. Eur. J.*, 2009, **15**, 186; (b) P. Pyykkö and M. Atsumi, *Chem. Eur. J.*, 2009, **15**, 12770; (c) P. Pyykkö, S. Riedel and M. Patzschke *Chem. Eur. J.*, 2005, **11**, 3511.

14 A.W. Addison, T.N. Rao, J. Reedijk, J. van Rijn, G.C. Verschoor, *J. Chem. Soc., Dalton Trans.* 1984, 1349. This criterion τ was obtained using Platon software. The value τ = 0 indicates the presence of ideal square pyramid, while τ = 1 for ideal trigonal bipyramid.

15 A.R. Sadique, M.J. Heeg and C.H. Winter, *Inorg. Chem.*, 2001, **40**, 6349.

16 T. Chivers, D.J. Eisler, C. Fedorchuk, G. Schatte and H.M. Tuononen, *Inorg. Chem.*, 2006, **45**, 2119.

17 V.L. Blair, W. Clegg, A.R. Kennedy, Z. Livingstone, L. Russo and E. Hevia, *Angew. Chem., Int. Ed.*, 2011, **50**, 9857.

18 For example see: R.J. Schwamm, B.M. Day, N.E. Mansfield, W. Knowelden, P.B. Hitchcock and M.P. Coles, *Dalton Trans.*, 2014, **43**, 14302.

19 S.P. Green, C. Jones and A. Stasch, *Science*, 2007, **318**, 1754.

20 M. J. Frisch, G. W. Trucks, H. B. Schlegel, G. E. Scuseria, M. A. Robb, J. R. Cheeseman, G. Scalmani, V. Barone, B. Mennucci, G. A. Petersson, H. Nakatsuji, M. Caricato, X. Li, H. P. Hratchian, A. F. Izmaylov, J. Bloino, G. Zheng, J. L. Sonnenberg, M. Hada, M. Ehara, K. Toyota, R. Fukuda, J. Hasegawa, M. Ishida, T. Nakajima, Y. Honda, O. Kitao, H. Nakai, T. Vreven, J. A. Montgomery, Jr., J. E. Peralta, F. Ogliaro, M. Bearpark, J. J. Heyd, E. Brothers, K. N. Kudin, V. N. Staroverov, T. Keith, R. Kobayashi, J. Normand, K. Raghavachari, A. Rendell, J. C. Burant, S. S. Iyengar, J. Tomasi, M. Cossi, N. Rega, J. M. Millam, M. Klene, J. E. Knox, J. B. Cross, V. Bakken, C. Adamo, J. Jaramillo, R. Gomperts, R. E. Stratmann, O. Yazyev, A. J. Austin, R. Cammi, C. Pomelli, J. W. Ochterski, R. L. Martin, K. Morokuma, V. G. Zakrzewski, G. A. Voth, P. Salvador, J. J. Dannenberg, S. Dapprich, A. D. Daniels, O. Farkas, J. B. Foresman, J. V. Ortiz, J. Cioslowski and D. J. Fox, *Gaussian 09*, *Revision B.01*, Gaussian, Inc., Wallingford CT, 2010.

21 A. D. Becke, J. Chem. Phys. 1993, **98**, 5648.

22 (a) T.H. Dunning, *J. Chem. Phys.* 1989, **90**, 1007; (b) D.E. Woon, T.H. Dunning, *J. Chem. Phys.* 1993, **98**, 1358.

23 (a) S. Grimme, *J. Comput. Chem.* 2004, **25**, 1463; (b) S. Grimme, *WIREs. Comput. Mol. Sci.*, 2011, **1**, 211.

24 Y. Zhao and D. G. Truhlar, *Theor. Chem. Acc.*, 2008, **120**, 215.

25 (a) A.D. Becke, *Phys. Rev. A* 1988, **38**, 3098; (b) J.P. Perdew, *Phys. Rev. B* 1986, **33**, 8822.

26 A. V. Marenich, C. J. Cramer, D. G. Truhlar, *J. Phys. Chem. B* 2009, **113**, 6378

27 (a) K. Wolinski, J. F. Hinton and P. Pulay, *J. Am. Chem. Soc.*, 1990, **112**, 8251; (b) R. Cheeseman, G. W. Trucks, T. A. Keith, and M. J. Frisch, *J. Chem. Phys.* 1990, **104**, 5497.

28 P. Coppens, in *Crystallographic Computing*, ed. F. R. Ahmed, S. R. Hall, and C. P. Huber, Copenhagen, Munksgaard 1970, 255–270.

29 A. Altomare, G. Cascarone, C. Giacovazzo, A. Guagliardi, M. C. Burla, G. Polidori, M. Camalli, *J. Appl. Crystallogr.*, 1994, **27**, 1045.

30 G. M. Sheldrick, SHELXL-97, A Program for Crystal Structure Refinement. University of Göttingen, Germany 1997.

31 A.L. Spek, *Acta Crystalllogr., Sect. A* 1990, **46**, C34.

The reactivity of bis(organoamino)phosphanes with magnesium(II) reagents is reported. The outcome of reactions is influenced by tautomeric H-shift in ligand backbones.